

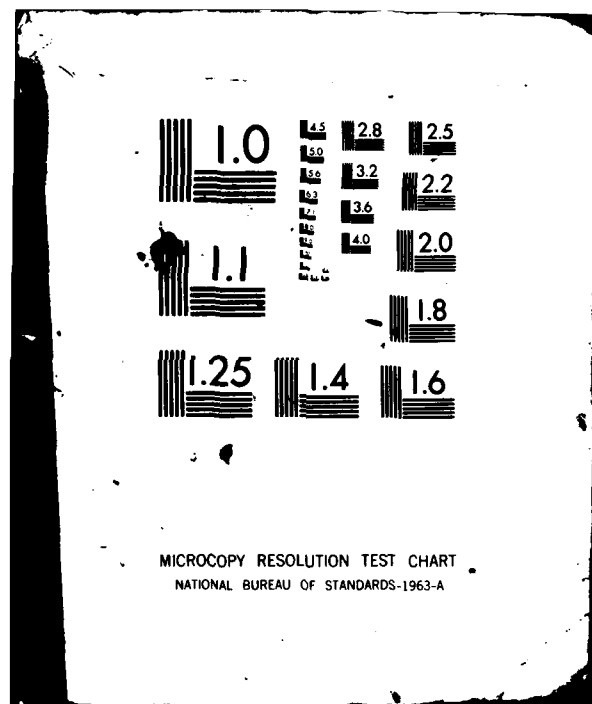
AD-A117 683

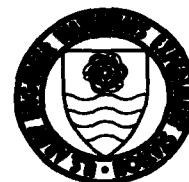
ARMY ENGINEER WATERWAYS EXPERIMENT STATION VICKSBURG--ETC F/G 4/2
OBJECTIVE SPECIFICATION OF ATLANTIC OCEAN WIND FIELDS FROM HIST--ETC(U)
MAY 82 D T RESIO, C L VINCENT, W D CORSON
WES/WIS-4

UNCLASSIFIED

NL

END
DATE
FILMED
8 82
DTIC





OBJECTIVE SPECIFICATION OF ATLANTIC OCEAN WIND FIELDS FROM HISTORICAL DATA

by

D. T. Resio, C. L. Vincent, W. D. Corson

Hydraulics Laboratory

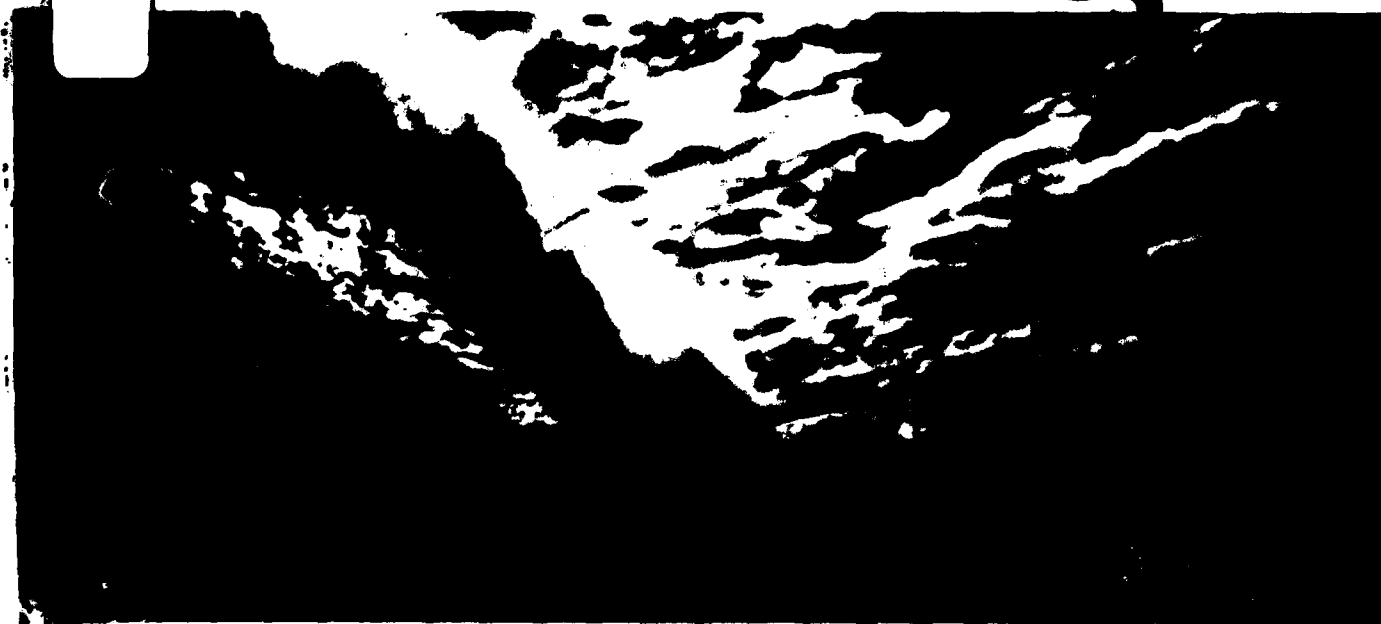
U. S. Army Engineer Waterways Experiment Station
P. O. Box 631, Vicksburg, Miss. 39180

WIS Report 4
May 1962

Approved For Public Release; Distribution Unlimited

DTIC
SELECTED
JUL 30 1982
H

AD A112443



WAVE INFORMATION STUDIES OF U.S. COASTLINES

FILE COPY

Prepared for Office, Chief of Engineers, U.S. Army
Washington, D.C. 20314

82 07 20 024

**Destroy this report when no longer needed. Do not return
it to the originator.**

**The findings in this report are not to be construed as an official
Department of the Army position unless so designated,
by other authorized documents.**

**The contents of this report are not to be used for
advertising, publication, or promotional purposes.
Citation of trade names does not constitute an
official endorsement or approval of the use of
such commercial products.**

**Cover photo by Steve Lissau. Photo originally ap-
peared in Oceanic, a publication of the Oceanic
Society, Vol. 12, No. 1, Jan-Feb 1978.**

12

Unclassified

SECURITY CLASSIFICATION OF THIS PAGE (When Data Entered)

REPORT DOCUMENTATION PAGE		READ INSTRUCTIONS BEFORE COMPLETING FORM
1. REPORT NUMBER WIS Report 4	2. GOVT ACCESSION NO. AD-A117683	3. RECIPIENT'S CATALOG NUMBER
4. TITLE (and Subtitle) OBJECTIVE SPECIFICATION OF ATLANTIC OCEAN WIND FIELDS FROM HISTORICAL DATA		5. TYPE OF REPORT & PERIOD COVERED Final report
		6. PERFORMING ORG. REPORT NUMBER
7. AUTHOR(s) D. T. Resio C. L. Vincent W. D. Corson		8. CONTRACT OR GRANT NUMBER(s)
9. PERFORMING ORGANIZATION NAME AND ADDRESS U. S. Army Engineer Waterways Experiment Station Hydraulics Laboratory P. O. Box 631, Vicksburg, Miss. 39180		10. PROGRAM ELEMENT, PROJECT, TASK AREA & WORK UNIT NUMBERS
11. CONTROLLING OFFICE NAME AND ADDRESS Office, Chief of Engineers U. S. Army Washington, D. C. 20314		12. REPORT DATE May 1982
		13. NUMBER OF PAGES 50
14. MONITORING AGENCY NAME & ADDRESS (if different from Controlling Office)		15. SECURITY CLASS. (of this report) Unclassified
		15a. DECLASSIFICATION/DOWNGRADING SCHEDULE
16. DISTRIBUTION STATEMENT (of this Report) Approved for public release; distribution unlimited.		
17. DISTRIBUTION STATEMENT (of the abstract entered in Block 20, if different from Report)		
18. SUPPLEMENTARY NOTES Available from National Technical Information Service, 5285 Port Royal Road, Springfield, Va. 22151.		
19. KEY WORDS (Continue on reverse side if necessary and identify by block number) Atlantic Ocean Water wave characteristics Deep water waves Wind (Meteorology) Mathematical models Numerical analysis Ocean waves		
20. ABSTRACT (Continue on reverse side if necessary and identify by block number) An integral part of the Wave Information Study's effort to hindcast 20 years of waves for U. S. coastlines is the reconstruction of surface wind fields from available historical meteorological data. This report presents the methodology utilized for the estimation of surface winds from pressure fields, air and sea-surface temperature fields, and observed winds from ships. A critical element in the evaluation of a numerical study such as this is an analysis of the estimated error characteristics of the results. (Continued)		


DTIC
ELECTED
JUL 30 1982
S H D

Unclassified

SECURITY CLASSIFICATION OF THIS PAGE(When Data Entered)

20. ABSTRACT. (Continued).

Extensive comparisons between observed and predicted winds are presented in the report. Without exception, these comparisons indicate that the statistical characteristics of the estimated winds provide a close approximation to those of the observed winds.



Unclassified

SECURITY CLASSIFICATION OF THIS PAGE(When Data Entered)

1 1

Preface

In late 1976, a study to produce a wave climate for U. S. coastal waters was initiated at the U. S. Army Engineer Waterways Experiment Station (WES). This Wave Information Study (WIS) was authorized by the Office, Chief of Engineers, U. S. Army, as a part of the Field Data Collection Program which is managed by the U. S. Army Coastal Engineering Research Center (CERC). The U. S. Army Engineer Division, South Atlantic, and the U. S. Army Engineer Division, New England, also authorized funds during the initial year of this study (FY 1978) to expedite execution of the Atlantic coast portion of this program.

This report, the fourth in a series, describes the techniques utilized to numerically hindcast oceanic wind fields and presents comparisons of the hindcast wind data and measured wind information. The study was conducted in the Hydraulics Laboratory under the direction of Mr. H. B. Simmons, Chief of the Hydraulics Laboratory, Dr. R. W. Whalin, Chief of the Wave Dynamics Division, Mr. C. E. Chatham, Jr., Chief of the Wave Processes Branch, and Dr. D. T. Resio, Research Physical Scientist and Project Manager. This report was prepared by Dr. D. T. Resio, Dr. C. L. Vincent, and Mr. W. D. Corson. Dr. Resio is presently employed by Oceanweather, Inc., Vicksburg, Mississippi; Dr. Vincent is currently employed by CERC, Fort Belvoir, Virginia.

Commanders and Directors of WES during the conduct of the study and the preparation and publication of this report were COL John L. Cannon, CE, COL Nelson P. Conover, CE, and COL Tilford Creel, CE. Technical Director was Mr. F. R. Brown.



Accession For	
NTIS GRA&I	<input checked="checked" type="checkbox"/>
DTIC TAB	<input type="checkbox"/>
Unannounced	<input type="checkbox"/>
Justification	
By	
Distribution/	
Availability Codes	
Dist	Avail and/or Special

Contents

	<u>Page</u>
Preface	1
Introduction	3
Estimation of Quasi-Geostrophic Winds	5
Direct Pressure Field Components	9
Estimation of Winds near the Surface	10
Comparison of Results	17
Summary and Conclusions	24
References	25
Appendix A: Comparison of Expected Errors in Wind Estimation With and Without Consideration of Stability and Baroclinicity in the Boundary Layer	A1
Appendix B: Site- and Time-Specific Comparisons	B1

OBJECTIVE SPECIFICATION OF ATLANTIC OCEAN
WIND FIELDS FROM HISTORICAL DATA

Introduction

1. The single most critical factor in calculating an oceanic wave climate by means of numerical models is the accurate estimation of wind fields and the associated momentum exchange from the atmosphere into the wave field. Report 1* in this series elaborated the procedure for obtaining representative pressure fields from historical data. This report discusses the methodology employed in converting these pressure fields into wind fields at the surface level. It is important to point out here that the approach used attempts to simulate the physics of synoptic-scale atmospheric motions to the degree permitted by our understanding of these phenomena. Consequently, there are no arbitrary constants that can be adjusted to "fit" the data in individual or composite comparisons. The success of this approach as indicated in the many comparisons to be presented demonstrates that although such models of the physics contain various assumptions implicit in their formulation, the estimated winds should be representative of actual wind conditions in any oceanic area. The possible exception to this would come in tropical areas where subsynoptic-scale phenomena become important and the geostrophic balance assumption becomes a poor approximation.

2. The type of wind specification used here plays an important role in the reconstruction of past individual meteorological and oceanographical events, such as surface waves and storm surges from severe extratropical cyclones. Similarly, in a probabilistic treatment of expected patterns of surface drift and associated environmental phenomena,

* W. D. Corson, D. T. Resio, and C. L. Vincent. 1980 (Jul). "Wave Information Study for U. S. Coastlines; Surface Pressure Field Reconstruction for Wave Hindcasting Purposes," Technical Report HL-80-11, Report 1, U. S. Army Engineer Waterways Experiment Station, CE, Vicksburg, Miss.

the dynamics of a system often must be related to long-term patterns of winds, waves, currents, and tides. It is frequently not sufficient to substitute a mean wind field into such a climatological-scale relationship. Instead, sequences of synoptic events with their wind field structures and related wind speeds, fetches, and durations must be considered. In viewing this problem of historical prediction for a wide range of potential applications, one must consider not only contamination of the final wind field due to modeling errors given accurate original data but also the propagation of errors in the original data through the model into the results. Thus, it is not always intuitively clear whether a more sophisticated or less sophisticated model will produce better results when applied to actual data, containing various types and magnitudes of errors.

3. Whereas wind fields in tropical storms have been represented in many studies by a small set of parameters, the complexity and diversity of shapes, intensities and internal structures of extratropical storms have precluded the use of parametric wind fields for these storms. In this report, tropical storms shall be excluded and attention restricted to the representation of past synoptic-scale extratropical systems.

4. Four primary sources of information were included in the assimilation of these wind fields:

- a. Gridded Northern Hemisphere pressure fields (Holl and Mendenhall 1971) (available from Navy Fleet Numerical Weather Central, Monterey, Calif.).
- b. North American Historical Weather Map Series (available from National Climatic Center, Asheville, N. C.).
- c. Surface marine observations (TDF-11 available from National Climatic Center, Asheville, N. C.).
- d. Airways surface observations (TDF-14 available from National Climatic Center, Asheville, N. C.).

Other than the weather maps, all of this information is available on magnetic tapes. It was decided to restrict attention first to computer processible forms of data and to include other sources of data if it were determined that these could lead to a significant improvement

in the accuracy of the final wind field.

5. Basically, two independent types of information in the four data sets are considered here--pressures and winds. The pressure data must first be converted, by means of an analysis of pressure gradients, into estimates of quasi-geostrophic winds. Then, these must be transformed into estimates of the wind vectors at some reference level near the surface. Only after this is it possible to combine the two sets of data, using some blending algorithm, into a single wind field.

Estimation of Quasi-Geostrophic Winds

6. All of the equations used in this report for the estimation of winds at the geostrophic level can be found in any basic meteorology text (for example, Hess 1959). Consequently, in this section, the mathematics will be omitted with the understanding that the equations for simple flows, which involve a balance of forces (geostrophic winds, gradient winds), baroclinic effects (thermal winds), and response to certain pressure field changes (isallobaric winds), can be found elsewhere.

7. Figure 1 shows, on a polar projection, the grid system on which pressure values were available. A preliminary check of the pressure fields in this data set and those in the weather map series revealed some large discrepancies between the two. As shown in Figure 2, the gridded data appear to misrepresent interiors of severe extratropical lows. A reduction of intensity of these systems was found to be typical of the gridded pressure data and probably represents a combination of the scale of the grid and the blending procedure used to smooth the pressure data. Actual surface observations show much better agreement with the weather map pressure fields; thus, it is presumed that the gridded data are in error. Given that this is the case, it would not be possible to obtain an accurate estimate of the geostrophic-level winds from the gridded pressure specification without some modification.

8. In the western Atlantic, cyclogenesis, rapid storm movement, and complexity of storm structure make it difficult to find a simple

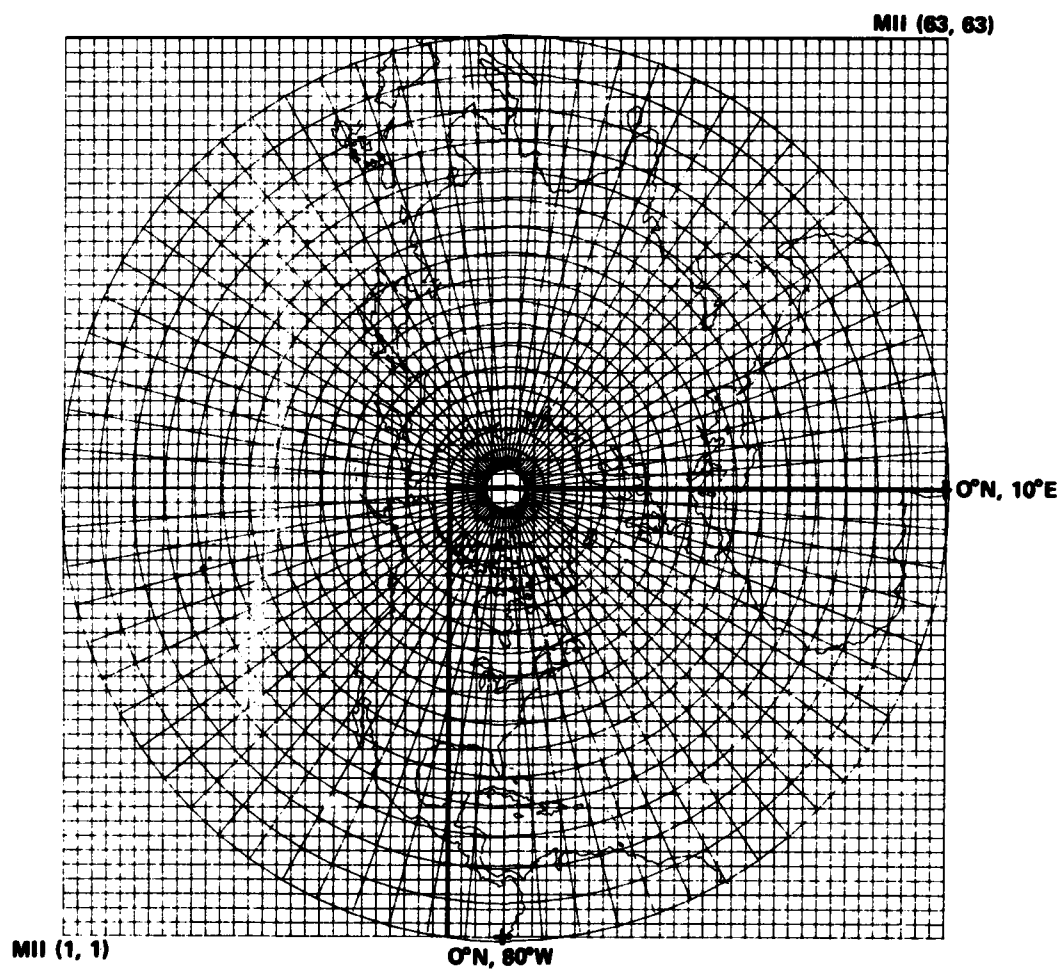


Figure 1. Meteorological International, Incorporated (MII),
63 × 63 grid on polar projection of the Northern Hemisphere

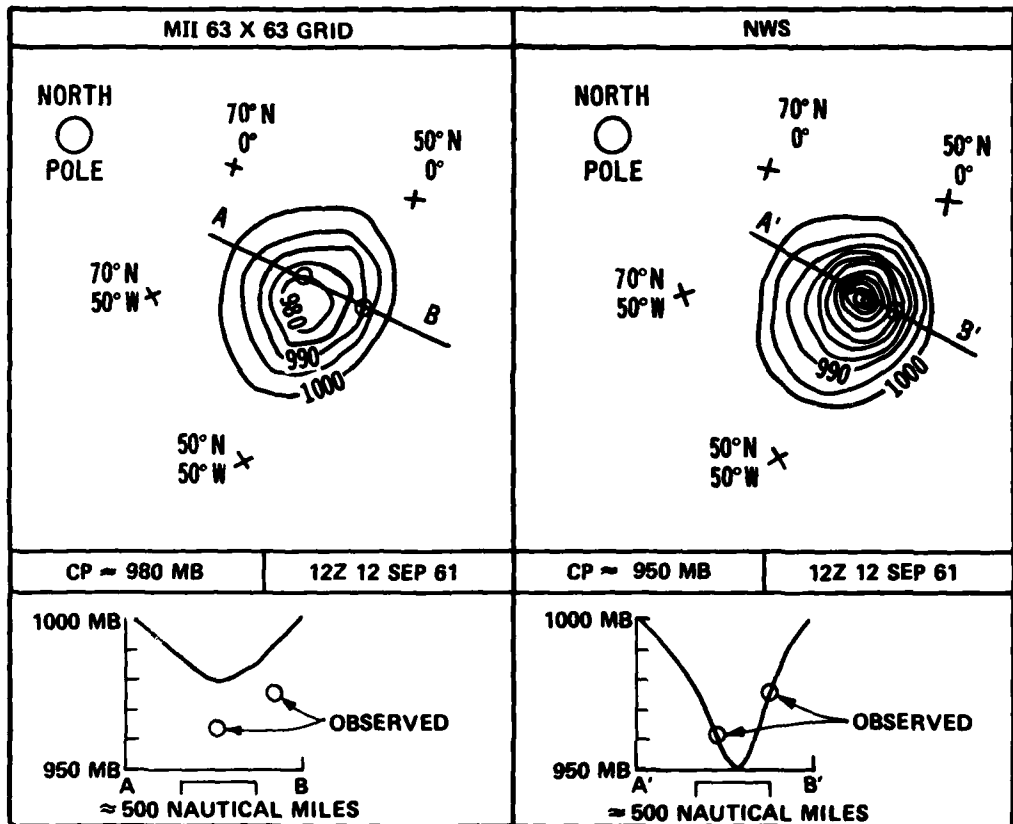


Figure 2. Contour of pressure field and cross section for MII data and National Weather Service (NWS) data

method for modifying the gridded data into pressure fields equivalent to those of the weather maps. For the area shown in Figure 3, weather maps

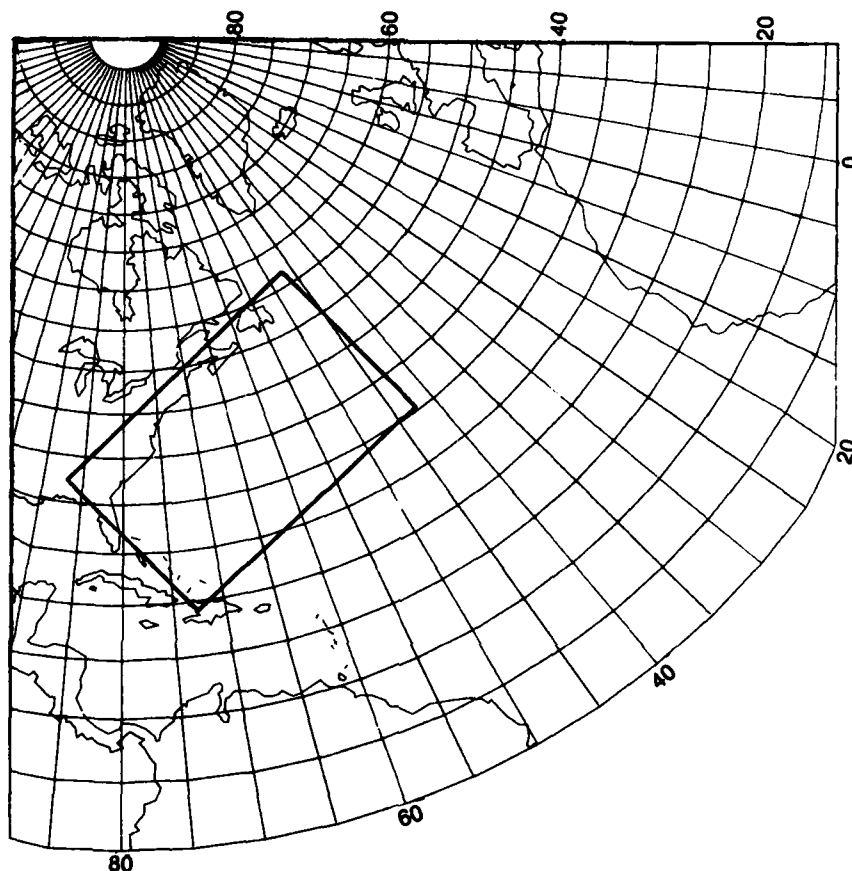


Figure 3. Map indicating area in which special attention was given to storms

(available at 6-hr intervals) were reviewed and those containing at least two closed contours within this area were machine-digitized. For storms outside of this area, a respecification of central pressure was used to amplify the pressure gradients in the storm interior. In order to maintain resolution of steep gradients, these respecified areas and digitized areas were blended into an interpolated pressure field on a grid with one-fourth of the spacing of the original grid (~30 NM).

Direct Pressure Field Components

9. Calculations of the surface wind fields were made in a coordinate system that consisted of great circle paths for quasi-east-west lines and orthogonals to the great circle paths for quasi-north-south lines (Figure 4). The reason for this was to have great circle paths for wave propagation into the east coast of the United States, our principal area of concern in this study. The basic methods could be applied to other coordinate systems after appropriate transformations.

10. The first approximation to the surface wind field in

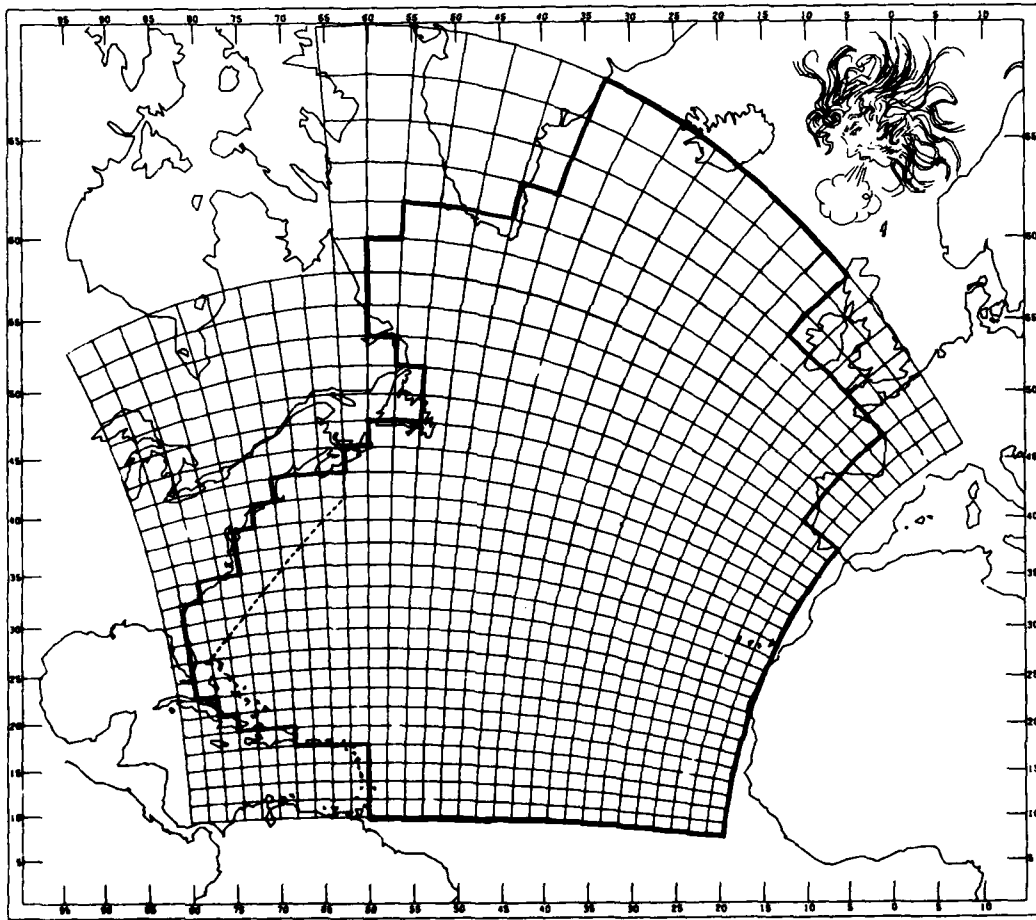


Figure 4. Wave Information Study's (WIS) spherical orthogonal grid on a Mercator projection. Heavy line is numerical boundary

nontropical regions is the geostrophic balance of pressure gradient and Coriolis force. The computer technique was designed to search for the local maximum pressure gradient across a particular grid point and to base the geostrophic wind speed and direction on this value. There are two major occasions where the surface wind field is influenced by the pressure field by components of a nongeostrophic nature. In tightly curved, low-pressure systems the effect of centrifugal accelerations modifies the pressure gradient-Coriolis force balance to produce lower geostrophic wind speeds. In such situations a gradient wind estimate was substituted for the geostrophic wind estimate. Both the geostrophic and gradient wind approximations are based on the presumption of balanced forces. Yet there are many times, particularly in the northern and western Atlantic, when the time rate of change of the pressure field is substantial and negates the balanced force assumptions. In these situations the isallobaric component of the wind field is estimated and included. A final consideration in the estimation of winds at the geostrophic level is the effect of horizontal temperature gradients. Such gradients introduce a thermal wind component into geostrophic-level winds. In order to compensate for this effect, the thermal wind equations were integrated up to a nominal level of 1000 m and this term was added to the resultant of the previous wind components.

Estimation of Winds near the Surface

11. In recent years, considerable research has gone into computing interactions between the free atmosphere and the planetary boundary layer. Since the scales considered in numerical, general circulation models cannot resolve fluxes of momentum, heat, and moisture from the surface, parametric methods are used in these models to couple the upper level flow to the earth's surface through the planetary boundary layer. The most successful methods of parameterizing fluxes in the boundary layer have evolved by means of matching solutions from similarity theories for an outer layer (Ekman region) and inner layer ("constant stress" region).

12. In a diabatic, baroclinic atmosphere Hess (1973) has shown that the flow in the boundary layer follows a nondimensional geostrophic departure function of the form

$$\frac{\vec{V}(z) - \vec{V}_g}{u_*} = \vec{F}\left(\frac{fz}{u_*}, \frac{u_*}{fL}, \frac{S_x}{f}, \frac{S_y}{f}\right) \quad (1)$$

where

\vec{V} = mean wind vector at any level, z , above the surface

\vec{V}_g = mean wind vector at the geostrophic level

\vec{F} = a universal function

u_* = friction velocity at the earth's surface

f = Coriolis acceleration

L = Obukhov length

S_x, S_y = components of the geostrophic wind shear

Introducing the following nondimensional parameters

$$\hat{\vec{V}} = \frac{\vec{V}}{u_*}$$

$$\hat{\vec{V}}_g = \frac{\vec{V}_g}{u_*}$$

$$\hat{S}_x = \frac{k^2 S_x}{f}$$

$$\hat{S}_y = \frac{k^2 S_y}{f}$$

$$\hat{z} = \frac{fz}{u_*}$$

$$\mu = \frac{ku_*}{fL}$$

where k is the von Karman constant, a solution for the winds in the boundary layer can be obtained in the form (Clarke and Hess 1974)

$$\ln R_o = A(\mu, \hat{S}_x, \hat{S}_y) - \ln \frac{u_*}{|\vec{V}_{g_o}|} + \left[\frac{k^2 |\vec{V}_{g_o}|^2}{u_*^2} - B^2(\mu, \hat{S}_x, \hat{S}_y) \right]^{1/2} \quad (2)$$

$$\sin \theta = \frac{Bu_*}{k |\vec{V}_{g_o}|} \quad (3)$$

where

$$R_o = \left(|\vec{V}_{g_o}| / fz_o \right) = \text{surface Rossby number}$$

z_o = surface roughness length

\vec{V}_{g_o} = surface geostrophic wind

θ = angle between the surface geostrophic wind and the surface stress

A, B = two nondimensional functions

13. Recent evidence (Kitaigorodskii and Volkov 1965, Smith and Banke 1975, Garratt 1977) suggests that z_o is not an external parameter for a water surface, but rather is an implicit function of momentum fluxes near the surface. Cardone* has revised his functional form of z_o (Cardone 1969) to be in agreement with the findings of Garratt (1977)

$$z_o = 0.1525 u_*^{-1} + 0.0144 u_*^2 - 0.00371 \quad (4)$$

(in cgs units). Equations 2, 3, and 4 along with an equation for the mean velocity profile in the "constant stress" region,

$$u(z) = \frac{u_*}{k} \left[\ln \left(\frac{z}{z_o} \right) - \psi \left(\frac{z}{L} \right) \right] \quad (5)$$

* Personal communication, 1977.

where ψ is a universal similarity function, provide a system of equations that can be solved iteratively for u_* , z_0 , and θ . The forms of ψ used in Equation 5 are the KEYPS formula (Lumley and Panofsky 1964) for unstable stratification and a log-linear function for stable stratification. Details of how typically recorded air temperature and sea temperature can be incorporated into these equations can be found in Cardone (1969).

14. The functions A and B in Equations 2 and 3 contain a dependence on both stability and geostrophic shear. Arya and Wyngaard (1975) demonstrated that these two factors can be considered independently and hence A and B can be written as

$$\begin{aligned} A &= A_s + A_b \\ B &= B_s + B_b \end{aligned} \tag{6}$$

where the subscripts s and b refer to effects of stability and baroclinicity, respectively. For a linearly decreasing shear to the top of a boundary layer scaled by u_*/f , the A_b and B_b terms integrated over the boundary layer thickness become

$$\begin{aligned} A_b &= k \frac{|\vec{H}|}{3} \cos \theta \\ B_b &= k \frac{|\vec{H}|}{3} \sin \theta \end{aligned} \tag{7}$$

where

\vec{H} = dimensionless thermal vector

θ = angle between the geostrophic wind and this vector

The operator \vec{H} is used here to define the horizontal temperature gradient at each point. The forms of the A_s and B_s terms are parameterized in terms of the dimensionless stability parameter μ ,

$$\left. \begin{aligned} A_s &= A_{s_o} [1 - \exp(0.015\mu)] \\ B_s &= B_{s_o} - (B_{s_o} - 0.23) [1 - \exp(0.03\mu)] \end{aligned} \right\} \mu \leq 0 \quad (8a)$$

$$\left. \begin{aligned} A_s &= A_{s_o} - 0.96\mu^{1/2} + \ln(\mu + 1) \\ B_s &= B_{s_o} + 0.7\mu^{1/2} \end{aligned} \right\} \mu > 0 \quad (8b)$$

Figure 5 shows a comparison of these parameterizations to field data from Clarke and Hess (1974). As seen here for $\mu > 0$, the A and B functions appear to approach asymptotic limits of about ± 15 in the field data; consequently, these limits were used in the PBL computer subroutine to replace calculated values greater than ± 15 . In this range the solution for the surface stress became insensitive to small

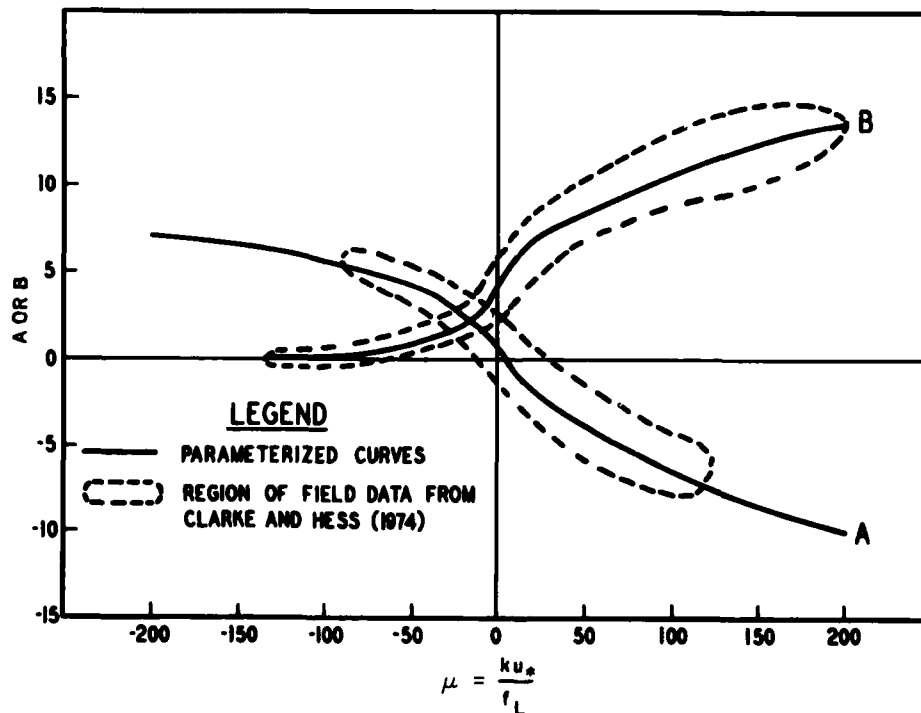


Figure 5. Comparison of parameterizations to field data (from Clarke and Hess 1974)

variations in A_s and B_s so the exact values become somewhat unimportant. This assumption ensures that no unreasonable magnitudes of μ come into the PBL routine and thus avoids potential problems with the numerical stability of the computations.

15. It should be noted that in this report the scale height used in the parameterization of the boundary layer is u_* / f and not the height of the inversion layer. Although this might lead to serious misrepresentations in boundary layers over land, over an open-ocean area it appears justifiable to retain a u_* / f scaling, due to much lower rates of surface heating and cooling. As with most assumptions of this nature, only results of extensive comparisons will demonstrate whether or not it is reasonable.

16. Given a specification of stability in terms of a temperature deviation between the water surface and the air at some reference level, the stability length can be estimated; and given a value for the horizontal temperature gradient in the surface layer, the thermal wind effects can be calculated. It should be immediately obvious that the quality of such estimates can be criticized. In fact, a primary concern in introducing a dependence on stability and baroclinicity into the wind estimation methodology is the possibility of large errors in the input thermal fields. However, rather than assume a priori that the information content of these estimates will negatively affect the accuracy of the wind calculations, it was decided to proceed on the hypothesis that the overall error in wind estimates would be reduced by inclusion of some measure of the horizontal and vertical thermal gradients in the planetary boundary layer.

17. In Appendix A a derivation of a comparison of inherent errors in wind fields, with and without consideration of thermal factors, is given. As indicated there, the less sophisticated approach does not guarantee better results on the basis of a lack of sensitivity to uncertain input parameters. Instead, the lack of consideration of persistent factors, such as the strong temperature gradients along the U. S. Atlantic coast, can introduce large regional biases in wind estimates. On the other hand, it is also important to avoid the introduction of large

local errors into objective schemes through the use of overly sensitive measures of thermal gradients. For example, if there is a sparse network of ships reports of surface temperatures and air-sea temperature differences, a single erroneous ship report can introduce significant errors into an estimate of thermal gradients over a relatively large area. Also, there will be times in some regions where no reliable information exists for a prolonged period of time. Since the hindcast effort for which these winds were needed extends over a 20-year interval (1956 through 1975), the effort required to remedy such situations would have been almost insurmountable. Thus, a different approach was needed.

18. After some analyses, it was determined that stable estimates of local surface temperature and air-sea temperature difference could be obtained by stratifying their variation with respect to time into two scales, seasonal and synoptic. Time of year, t^* , sufficed to give a good measure of the former scale of variation; and the direction of the geostrophic wind, α , provided a reasonable measure of the flux of air from different source regions on a synoptic-scale. Hence, the air temperature, T_a , and air-sea temperature difference, T_{a-s} , could be characterized by two parameters. To obtain a reliable estimate of T_a and T_{a-s} , the total sample of ships observations for four 5-year periods was used to define these variables for each month of the year for each 10-deg wind direction category. For each oceanic grid point shown in Figure 4, these two-dimensional matrices were calculated. Each thermal field constructed in this manner (as a function of t^* and α) was smoothed after the initial estimate to further reduce the possibility of extreme gradients over one or two grid points.

19. After the geostrophic-level winds were reduced to near-surface winds, independent observations from ships were blended into the wind fields. The procedure used was simply to average the observed wind speed with the nearest grid point wind speed. Although more sophisticated methods were considered, the effects due to differences in storm position seemed to offset any potential gain inherent in a more elaborate methodology. Wind directions from ships were not blended into the wind fields since a 180-deg direction error can be quite common due to

the manner in which the values are coded. Over the 20-year period for which calculations were made, approximately 7.4 million ships observations were averaged into the final wind fields.

Comparison of Results

20. In order to investigate whether or not the wind fields being calculated provide a reasonable representation of actual conditions, extensive comparisons between predicted winds and independent observations have been made. Three primary sources of data were involved in these comparisons: recorded data from NDBO (NOAA (National Oceanic and Atmospheric Administration) Data Buoy Office) buoys, Sable Island anemometer, and ships observations (before the information from these observations was blended into the wind fields). Along the Atlantic coast, hourly measurements of wind speed and direction at the 10-m elevation from the buoys afford an excellent opportunity to check the details of winds through time at a specific point. To establish the validity of the wind estimation procedure over the entire Atlantic Ocean, analyses must be made on the basis of comparisons within different portions of the Atlantic Ocean. The only data presently available that can provide good coverage over the entire Atlantic Ocean are ships observations. Unfortunately, most of the observations made in the Atlantic Ocean are visual estimates of wind speeds and directions rather than instrument measurements; therefore, any comparisons made to them must consider the effects of biases and random errors in the visual observations.

21. As previously stated, the available observed data sets are different in nature, i.e., the ships data are for relatively long periods of time and cover the Atlantic Ocean (nonspecific), while buoy or platform data are more specific in time and space (specific). The nonspecific ships data will be compared in this section and comparisons to specific information will be presented in Appendix B. Also, the comparisons to ships wind speed will be discussed first, and then the comparisons of wind direction will be presented.

22. Before an estimate of the random error can be obtained, bias

present in the ships observations must be removed to whatever extent possible. Cardone (1969) summarizes previous investigations of bias in winds reported by ships by the following formula (in knots):

$$w = 2.16 w_r^{7/9} \quad (9)$$

where

w = corrected wind speed

w_r = reported wind speed

Unless otherwise stated, this relationship was used to transform ships wind speeds prior to comparison to predicted wind speeds.

23. The magnitude of random errors in ships observations of wind speed can be estimated from comparisons to some known standard such as an NDBO buoy. Figure 6 shows the results of such a comparison. As is typical of this type of environmental data, the random error is not homoscedastic, but rather has a dependence on the magnitude of the

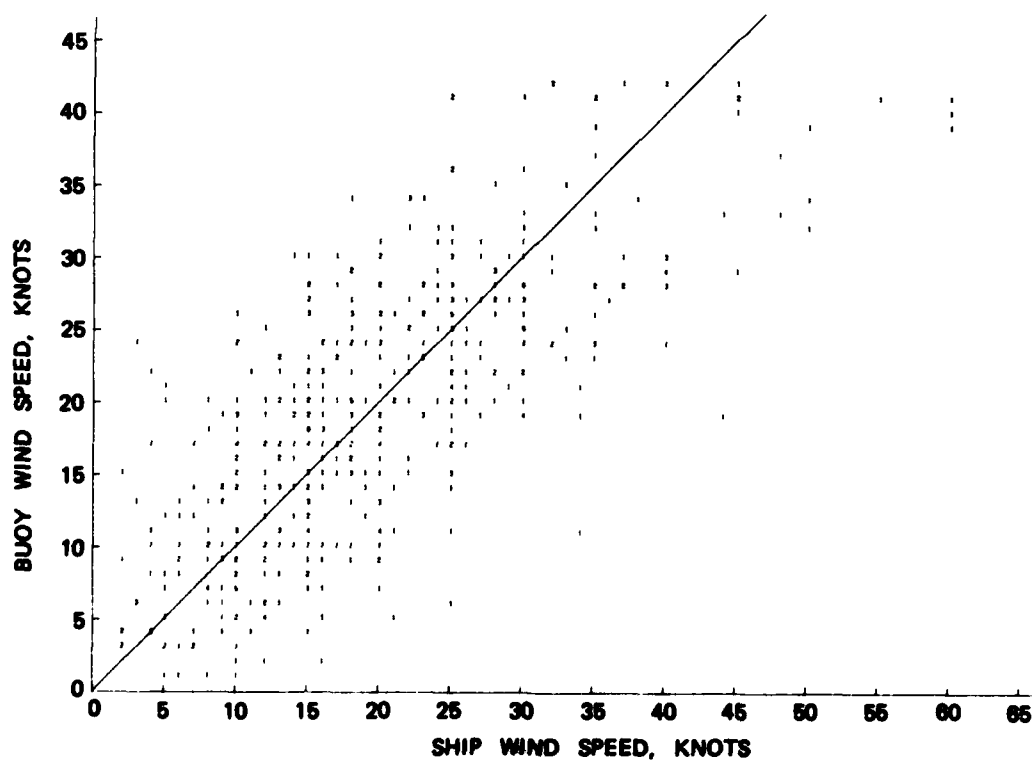


Figure 6. Crossplot of buoy wind speeds and ship wind speeds for one year

variate. Consequently, if a comparison between our predicted wind speeds and ships observations is made, the apparent error variance, σ_a^2 must be stratified by velocity class in order to be able to estimate its two components, error due to incorrect predictions, σ_p^2 , and error due to inaccurate observations, σ_o^2 . The estimate of error in predicted winds obtained in this fashion can be written as

$$\sigma_p(u) = \left[\sigma_a^2(u) - \sigma_o^2(u) \right]^{1/2} \quad (10)$$

where σ_o^2 , determined independently from comparisons of ships winds to buoys, is approximated by $\sigma_o^2 = 1.5 + 0.18 \bar{u}$, where \bar{u} is the sample mean of the wind speeds.

24. From comparisons to buoys and using Equation 10 for comparisons to ships observations it is seen that there is an apparent dependence on wind speed of the standard deviation of the error distribution which is approximately by the linear relation

$$\sigma_p = 1.7 + 0.11 \bar{u} \quad (11)$$

where

\bar{u} = average recorded wind speed in the comparisons

σ = standard deviation of the errors

This error compares well with reported error values in Overland and Gemmill (1977). In that study a limited area, fine-mesh model was used to obtain pressures and wind speeds at the geostrophic level over the New York Bight. The best results for surface winds were obtained with a PBL model (Cardone 1969) approach, producing σ values of 2.92 m/sec, 3.49 m/sec, and 2.93 m/sec for $u < 5$, $5 < u < 10$, and $u > 12.5$ m/sec wind speed classes, respectively.

25. Figures 7, 8, and 9 present three separate comparisons of ships and predicted wind speeds. The distribution of deviations is displayed in Figure 7. Figure 8 shows contoured densities for a cross plot of predicted wind speeds and observed ships winds before correction through Equation 9 for all cases in 1974. Comparison parameters from the January, April, July, and October months were calculated from the

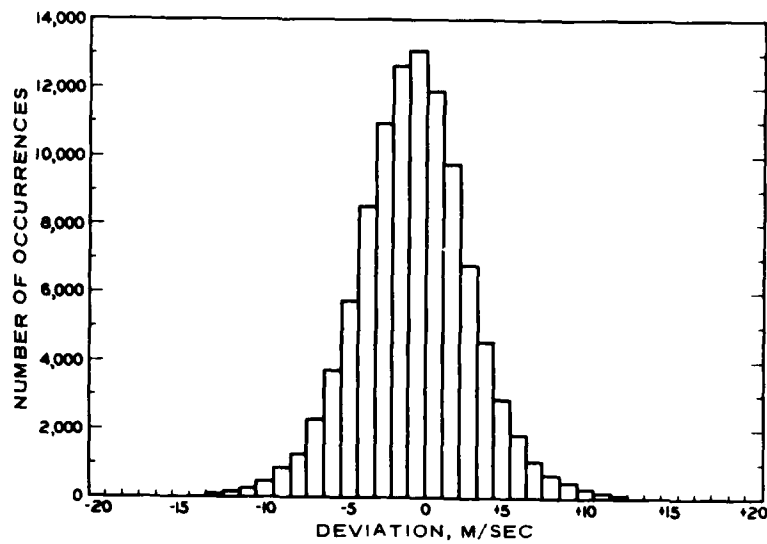


Figure 7. Deviation of computed wind speeds (grid) from measured wind speeds (ships) for one year

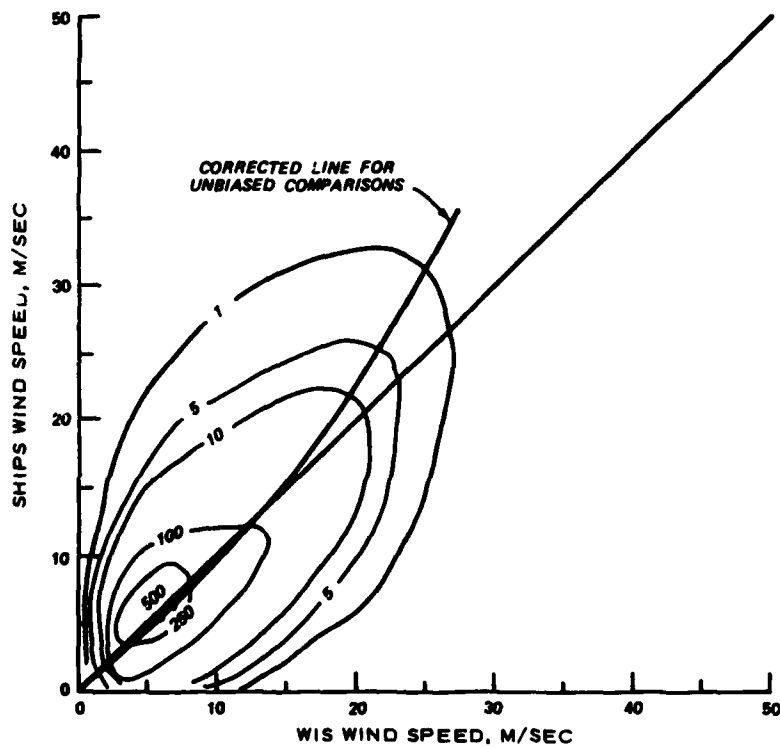


Figure 8. Joint distribution of paired observations of observed (ships) wind speeds and predicted (WIS) wind speeds

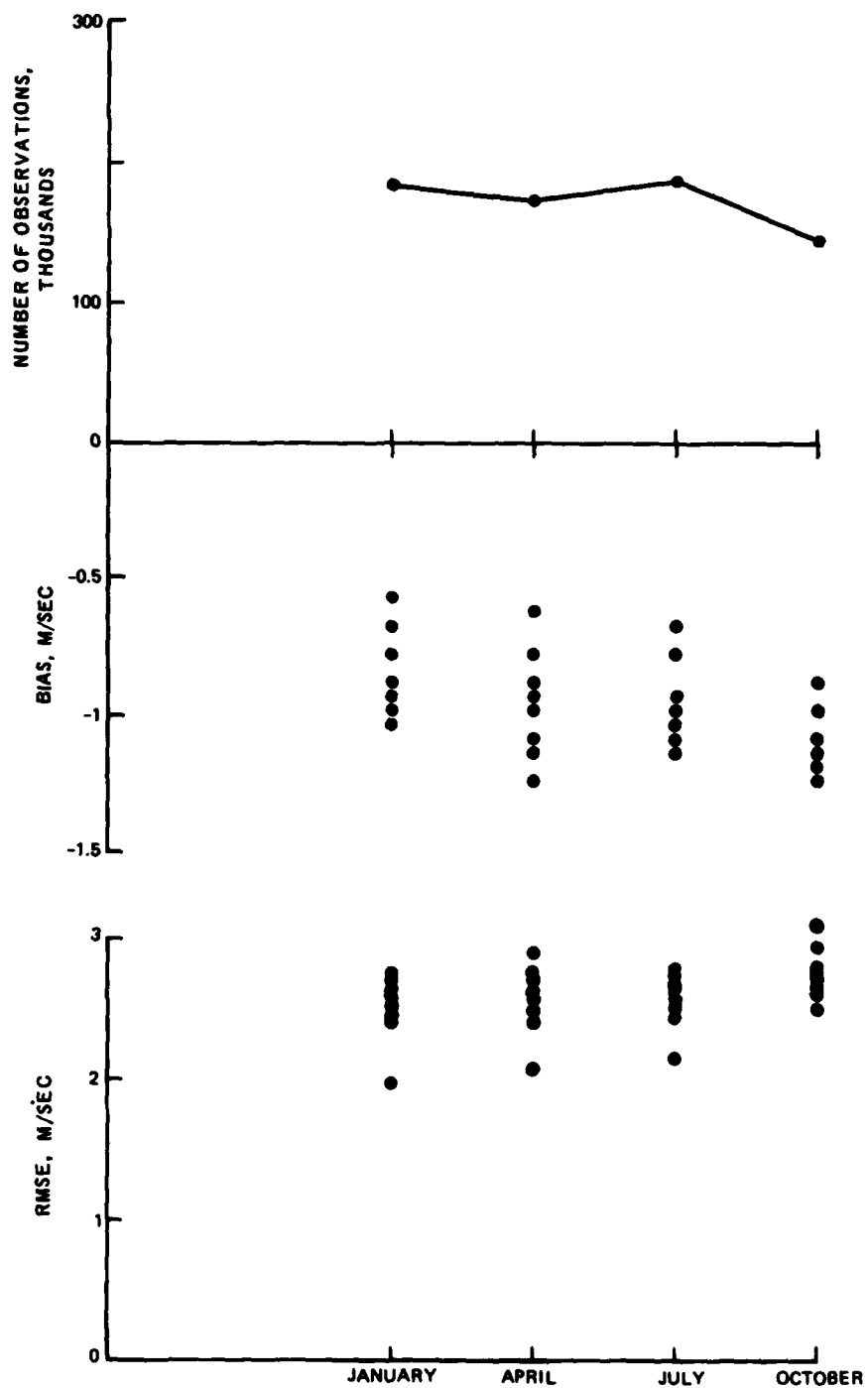


Figure 9. Bias and root-mean-square error (RMSE) of wind speed for the months indicated. Information was computed for 10 years of each month (some dots overlay each other)

20 years of information and are presented in Figure 9.*

26. Since the results show the same type of observer bias as given independently by Equation 9, they indicate that there is little apparent bias in the wind speed estimates across the Atlantic Ocean.

27. As shown in Figure 10, there does not appear to be significant bias in predicted wind directions when compared with ships observations. Thus, the wind field estimation methodology outlined in this paper seems to provide a good synoptic-scale description of actual wind fields over the entire Atlantic Ocean.

28. It should be noted that in our comparisons the random error in wind directions decreases markedly with increasing wind velocity. Upon inspection, it appears that much of the deviation between observed and predicted wind speeds and directions is due to differences in storm locations. Time-series plots of simulated winds often exhibited lags or leads of 6 hours or so compared with nearby measurements. Since winds tend to be less well organized under low wind speed conditions, and hence more highly variable, it is expected that such conditions will produce larger errors in wind direction. An additional factor to consider in these comparisons is that noninstrumented estimates of wind direction appeared to be highly dependent of wind speed.

29. It was mentioned near the beginning of this report that we would reconsider our decision to include only large data sets in machine-processible form, based on our final result. Our primary interest in this study is a region along the east coast of the United States, where a high density of ships observations prevailed during the 20-year interval of interest. After reviewing the results obtained in this methodology and considering the large number of data already included, it is doubtful that any small set of additional data will strongly influence the estimated wind fields. Consequently, the decision was made not to process additional data for inclusion into the wind fields as a part of this study. This is not intended to imply that some

* The years, from which the months were chosen, were randomly selected. The parameters of each averaged month are intended to approximate seasonal information.

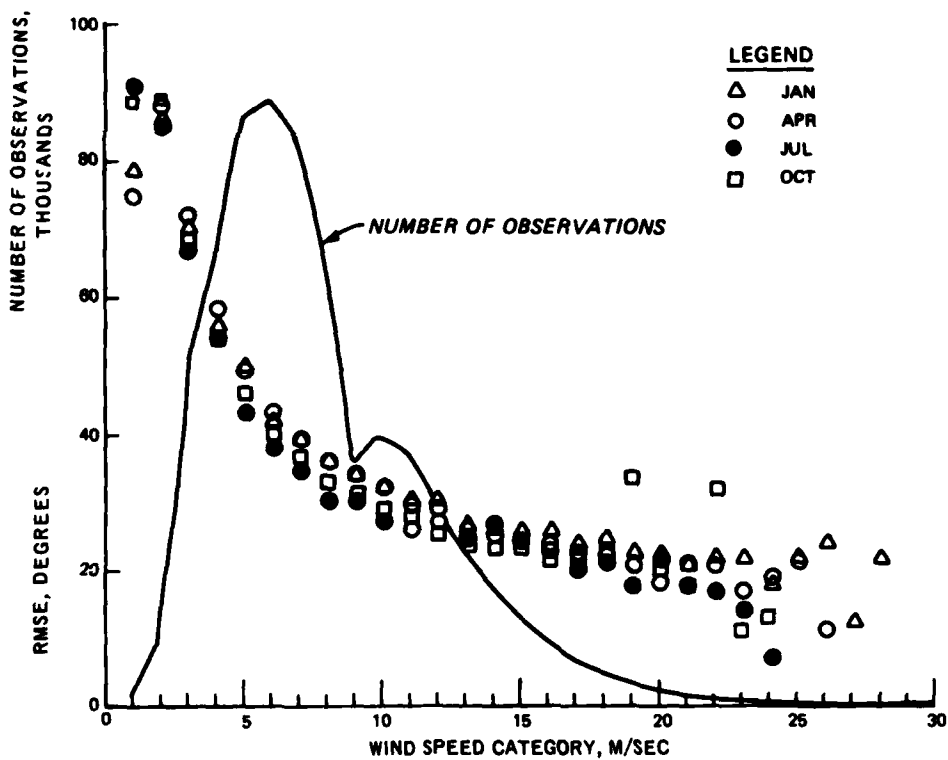
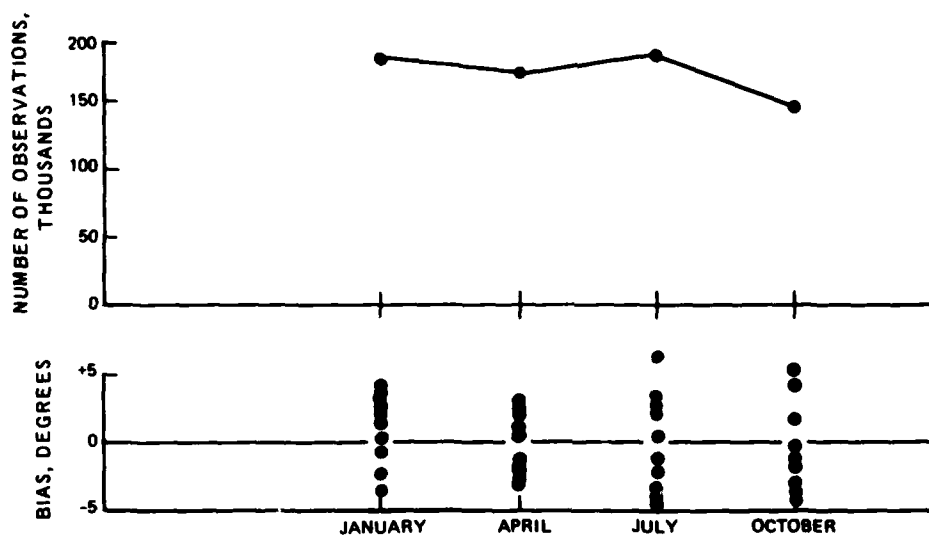


Figure 10. Bias and RMSE of predicted wind direction. Information was selected as in Figure 9

local improvement in these wind field estimates may not be obtainable by blending in some specialized data source not included here.

Summary and Conclusions

30. An objective method for obtaining wind fields has been developed and 20 years of wind fields covering most of the North Atlantic Ocean have been calculated. This method uses historical information on pressure fields and horizontal thermal gradients to obtain an estimate of the wind vector at the geostrophic level. A parametric representation of the planetary boundary layer, based on similarity theory, is used to reduce this wind to a surface wind vector. Input parameters in terms of atmospheric stability and baroclinicity are developed from a statistical analysis of their dependence on the wind at the geostrophic level. Comparison of predicted winds to observed winds indicates that the methodology used here produces relatively unbiased winds with a scalar RMSE slightly dependent on wind speed ($\sigma_p = 1.7 + 0.11 \bar{u}$ m/sec where \bar{u} is the mean wind speed of the sample).

31. The hindcast wind fields have been used in a wave hindcast program to generate wave data for the North Atlantic Ocean (Corson et al. 1980). Comparisons of the hindcast wave data and measured wave data indicate good agreement between the two data sets (Corson and Resio 1981). Thus, it is apparent that the methods employed to generate the 20 years of wind fields were appropriate.

References

- Arya, S. P. S., and Wyngaard, J. C. 1975. "Effect of Baroclinity on Wind Profiles and the Geostrophic Drag Law for the Convective Planetary Boundary Layer," J. Atmos. Sci., American Meteor. Soc., Boston, Mass., Vol 32, pp 767-778.
- Cardone, V. J. 1969. "Specification of the Wind Distribution in the Marine Boundary Layer for Wave Forecasting," Tech. Rept. 69-1. Geophys. Sci. Lab., New York University.
- Clarke, R. H., and Hess, G. D. 1974. "Geostrophic Departure and the Functions A and B of Rossby - Number Similarity Theory," Boundary Meteorology 7, Reidel Publ. Co., Dordrecht-Holland, pp 267-287.
- Corson, W. D., et al. 1980 (Jan). "Atlantic Coast Hindcast, Deepwater, Significant Wave Information," Wave Information Study Report 2, U. S. Army Engineer Waterways Experiment Station, CE, Vicksburg, Miss.
- Corson, W. D., and Resio, D. T. 1981 (May). "Comparisons of Hindcast and Measured Significant Wave Heights," Wave Information Study Report 3, U. S. Army Engineer Waterways Experiment Station, CE, Vicksburg, Miss.
- Garrett, J. R. 1977. "Review of Drag Coefficients over Oceans and Continents," Mon. Wea. Rev., Vol 105, pp 915-929.
- Hess, G. D. 1973. "On Rossby - Number Similarity Theory for a Baroclinic Planetary Boundary Layer," J. Atmos. Sci., American Meteor. Soc., Vol 30, pp 1722-1723.
- Hess, Seymour L. 1959. Introduction to Theoretical Meteorology, Holt, Rinehart and Winston, New York.
- Holl, Manfred M., and Mendenhall, Bruce R. 1971. The FIB Methodology and Application, Meteorology International, Inc., Monterey, Calif.
- Kitaigorodskii, S. A., and Volkov, Y. A. 1965. "On the Roughness Parameter of the Sea Surface and the Calculation of Momentum Flux in the Water Layer of the Atmosphere," Izv. Atm. and Ocean. Phy., Ser. 1, 973-988.
- Lumley, J. L., and Panofsky, H. A. 1964. The Structure of Atmospheric Turbulence, Wiley, New York.
- Overland, H., and Gemmill, W. 1977. "Specification of Marine Winds in the New York Bight," Mon. Wea. Rev., Vol 105, pp 1003-1008.
- Smith, S. D., and Banke, E. G. 1975. "Variation of the Sea Surface Drag Coefficient with Wind Speed," J. R. Met. Soc., Vol 101, pp 665-673.

Appendix A: Comparison of Expected Errors in Wind Estimation
With and Without Consideration of Stability and
Baroclinicity in the Boundary Layer

1. Neglecting subsynoptic-scale perturbations in the wind field, recent experimental evidence and theoretical treatments indicate that the wind near the surface should be primarily a function of five factors, the geostrophic wind vector (\vec{G}), the thermal wind vector ($\overline{\nabla_h T}$), vertical temperature gradients near the surface ($\overline{\nabla_z T}$), the Coriolis acceleration (f), and the roughness of the surface (z_0) (Cardone 1969*). A "true" functional relation for the surface wind vector thus could be put in the form

$$\vec{w} = \vec{w}(\vec{G}, \overline{\nabla_h T}, \overline{\nabla_z T}, f, z_0) \quad (A1)$$

In looking for an optimal wind estimator, we are generally looking to minimize two error terms, bias and random error,

$$b = E [\vec{w} - \vec{w}_e] \quad (A2)$$

$$\sigma^2 = E [(\vec{w} - \vec{w}_e)^2] \quad (A3)$$

where

b, σ^2 = expected bias and error variance, respectively

$E []$ = expectation operator

\vec{w}_e = estimated wind vector near the surface

Given two estimators, one which considers only a dependence on \vec{G} and f and a second which considers all five primary factors, i.e.

$$\vec{w}_1 = \vec{w}_1(\vec{G}, f) \quad (A4)$$

$$\vec{w}_2 = \vec{w}_2(\vec{G}, \overline{\nabla_h T}, \overline{\nabla_z T}, f, z_0) \quad (A5)$$

then b and σ^2 can be defined in terms of integrals over a

* See References at end of main text.

multidimensional probability space. If the relation for w_1 is considered to be a "true" relation for neutral conditions, we have for the case $\langle \vec{G}, \vec{\epsilon}_G \rangle = 0$

$$b_1 \approx \int \dots \int (\vec{w} - \vec{w}_1) p(\vec{\epsilon}_G, \vec{v}_h, \vec{v}_z, z_o) d\vec{\epsilon}_G d(\vec{v}_h) d(\vec{v}_z) dz_o \quad (A6)$$

$$\sigma_1^2 \approx \int \dots \int (\vec{w} - \vec{w}_1)^2 p(\vec{\epsilon}_G, \vec{v}_h, \vec{v}_z, z_o) d\vec{\epsilon}_G d(\vec{v}_h) d(\vec{v}_z) dz_o \quad (A7)$$

where $\vec{\epsilon}_G$ is a random vector describing the error between a specified value of \vec{G} and the true value of \vec{G} . If we allow a similar set of random error vectors to characterize the errors of four of the input parameters, with $\langle \vec{G}, \vec{\epsilon}_G \rangle \equiv \langle \vec{v}_h, \vec{\epsilon}_{v_h} \rangle \equiv \langle \vec{v}_z, \vec{\epsilon}_{v_z} \rangle \equiv \langle z_o, \vec{\epsilon}_{z_o} \rangle \equiv 0$, and assume that the underlying relation for \vec{w}_2 is approximately correct, then we obtain for b_2

$$b_2 = \int \dots \int (\vec{w} - \vec{w}_2) p(\vec{\epsilon}_G, \vec{\epsilon}_{v_h}, \vec{\epsilon}_{v_z}, \vec{\epsilon}_{z_o}) d\vec{\epsilon}_G d\vec{\epsilon}_{v_h} d\vec{\epsilon}_{v_z} d\vec{\epsilon}_{z_o} \quad (A8)$$

and for σ_2^2

$$\sigma_2^2 = \int \dots \int (\vec{w} - \vec{w}_2)^2 p(\vec{\epsilon}_G, \vec{\epsilon}_{v_h}, \vec{\epsilon}_{v_z}, \vec{\epsilon}_{z_o}) d\vec{\epsilon}_G d\vec{\epsilon}_{v_h} d\vec{\epsilon}_{v_z} d\vec{\epsilon}_{z_o} \quad (A9)$$

The important distinction between the integrals in A6 and A7 and A8 and A9 is that the former are defined over ranges in input variables ($d\vec{v}_h, d\vec{v}_z, dz_o$) as well as over a range in the random vector ($d\vec{\epsilon}_G$), whereas the latter are defined over the ranges only of the random vectors ($d\vec{\epsilon}_G, d\vec{\epsilon}_{v_h}, d\vec{\epsilon}_{v_z}, d\vec{\epsilon}_{z_o}$). Thus, the \vec{w}_1 estimates, which are typical of winds predicted by regression method (i.e. $|\vec{w}| = \lambda |\vec{G}|$), where λ is a constant for a specific latitude, can contain large biases when applied

in regions where the means $\overline{\vec{v}_h T}$ and $\overline{\vec{v}_z T}$ are not equal to zero or where \bar{z}_0 is different from the z_0 for which the statistical method was calibrated. For example, over the entire Atlantic Ocean, the average stability is near neutral and the average baroclinicity is small; however, near the east coast of North America strongly baroclinic, unstable conditions persist during the winter.

2. Similarly, the σ_1^2 term contains contributions from the neglect of the $\overline{\vec{v}_h T}$, $\overline{\vec{v}_z T}$, z_0 terms. If the dispersions of the distributions of these variables $\left(E \left[(\overline{\vec{v}_h T} - \overline{\vec{v}_h T})^2 \right], \text{ etc.} \right)$ are larger than random errors in the specification of $\vec{w}_2 \left(E \left[\epsilon_{\vec{v}_h T}^2 \right], \text{ etc.} \right)$ then we should have $\sigma_1^2 > \sigma_2^2$. Since the variations in $\overline{\vec{v}_h T}$ and $\overline{\vec{v}_z T}$ include contributions from synoptic scales up through seasonal scales of atmospheric circulation, they can indeed be quite large at a given site.

3. On the other hand, if the dependence of \vec{w}_2 on the input variables is almost linear or if the dependence is symmetric with respect to a perturbation around a "true" value, i.e.

$$\vec{w}_2 \approx \frac{1}{2} \sum_{k=1}^2 \vec{w}_2 \left[\vec{G} + (-1)^k \epsilon_G, \overline{\vec{v}_h T} + (-1)^k \epsilon_{\overline{\vec{v}_h T}}, \overline{\vec{v}_z T} + (-1)^k \epsilon_{\overline{\vec{v}_z T}}, f, z_0 + (-1)^k \epsilon_{z_0} \right]$$

b_2 should be quite small. This condition is very nearly met for the boundary layer operators for typical ϵ -values. Since in the boundary layer parameterization here, z_0 is an implicit function of the surface stress ($\sim u_*^2$), its error properties are included in the effects of errors in specifications of \vec{G} . This brings out an interesting point since a $|\vec{w}_1| = \lambda |\vec{G}|$ relation does not contain this implicit dependence on z_0 ; hence, the assumption made earlier that such a form could represent a "true" relation for neutral conditions is not strictly valid.

4. Although the method used here to compare expected bias and

random errors seems laborious, it does provide a means of addressing a somewhat complex question. The use of overly simple methodologies is often appealing in terms of convenience; however as indicated here, methods which better represent boundary layer effects should consistently provide a less-biased estimate of the surface wind. Also, under most circumstances, the PBL approach, including thermal effects and an implicit dependence of z_0 on the surface stress, should produce less random error than the neglect of these factors.

Appendix B: Site- and Time-Specific Comparisons

1. In a previous section of this report extensive comparisons to ships observations were presented. These comparisons showed the predicted winds to be valid over the entire Atlantic Ocean. In this section, site- and time-specific comparisons are employed to further investigate characteristics of the wind hindcast procedure.

2. Reliable, recorded wind data were available from three sites when these comparisons were performed*: Sable Island, NDBO buoy EB01, and NDBO buoy EB13 (Figure B1). Data from each site were compared with

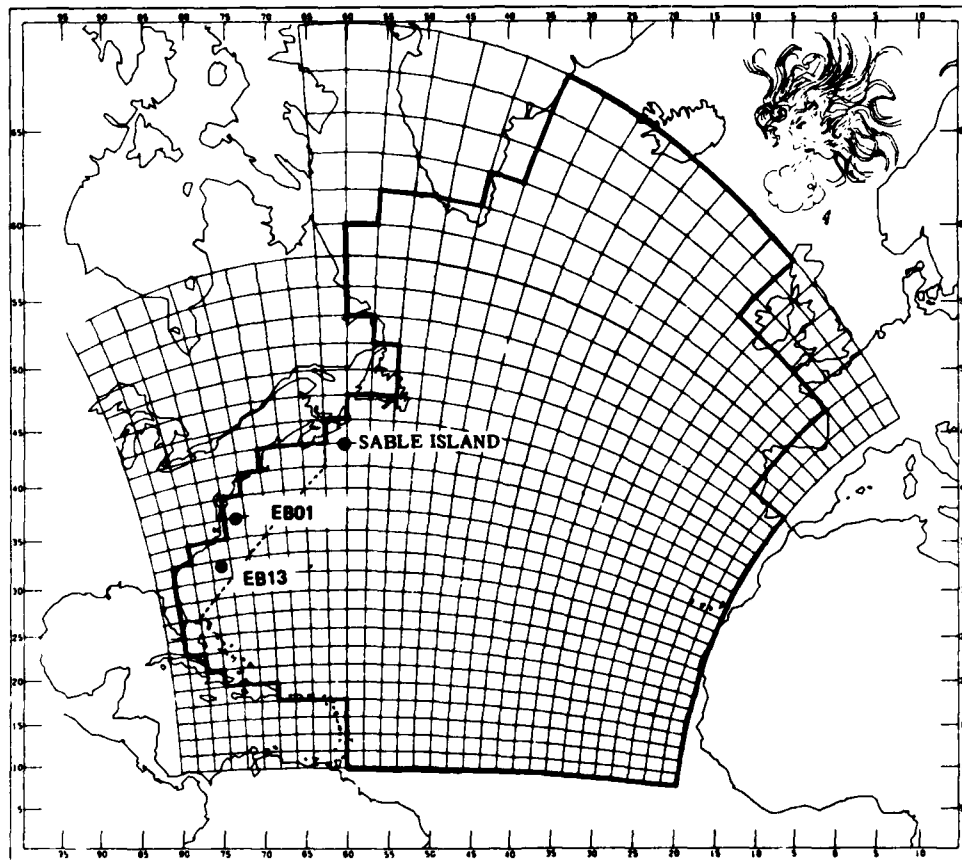


Figure B1. Location map for available recorded data site

* All comparisons have been adjusted to comparable anemometer heights.

data from the nearest Wave Information Study (WIS) grid point.

3. The wind comparisons at Sable Island were performed after first transforming the Sable Island winds to the hypothetical 19.5-m level of the WIS winds. Figures B2-B6 indicate that the wind hindcast data are in phase with the measured data at Sable Island and the hindcast procedure produces winds of similar magnitudes as the measured data. Additionally, Figures B7 and B8 show no apparent bias in the predicted winds at Sable Island.

4. To better describe how well the hindcast procedure performed for high wind conditions, computed and measured cases were compared for each event in which wind speeds over 30 knots were recorded at Sable

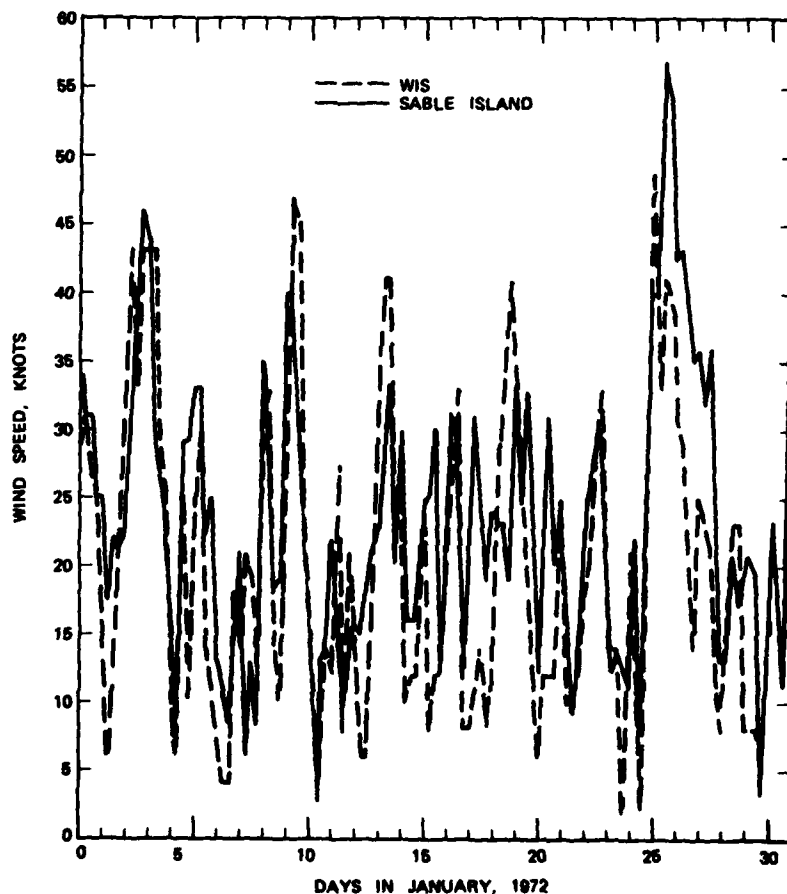


Figure B2. Comparison of hindcast (WIS) and measured (Sable Island) wind speed at Sable Island for January 1972

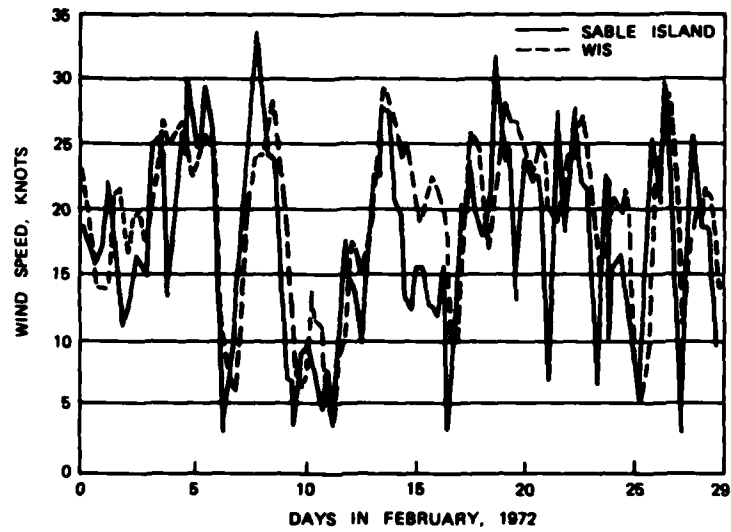


Figure B3. Comparison of hindcast (WIS) and measured (Sable Island) wind speed at Sable Island for February 1972

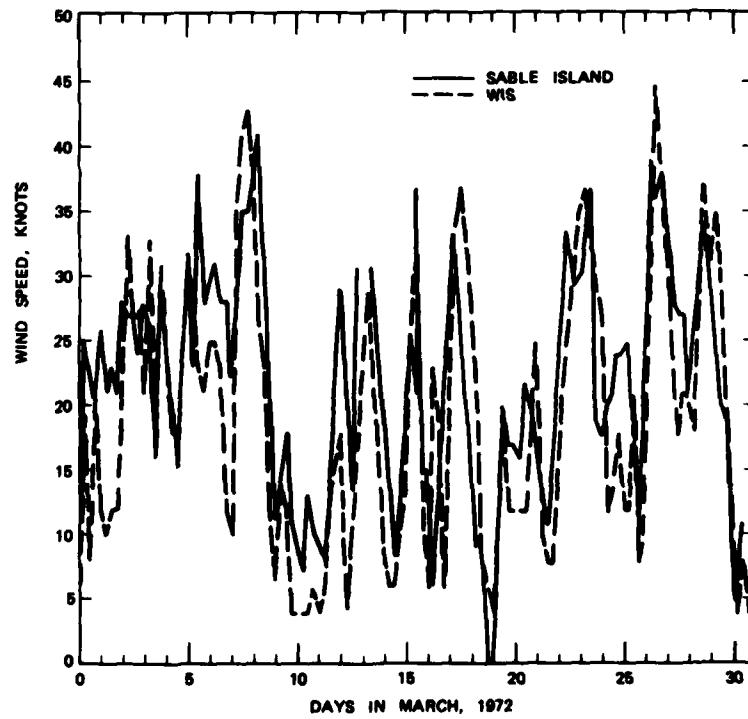


Figure B4. Comparison of hindcast (WIS) and measured (Sable Island) wind speed at Sable Island for March 1972

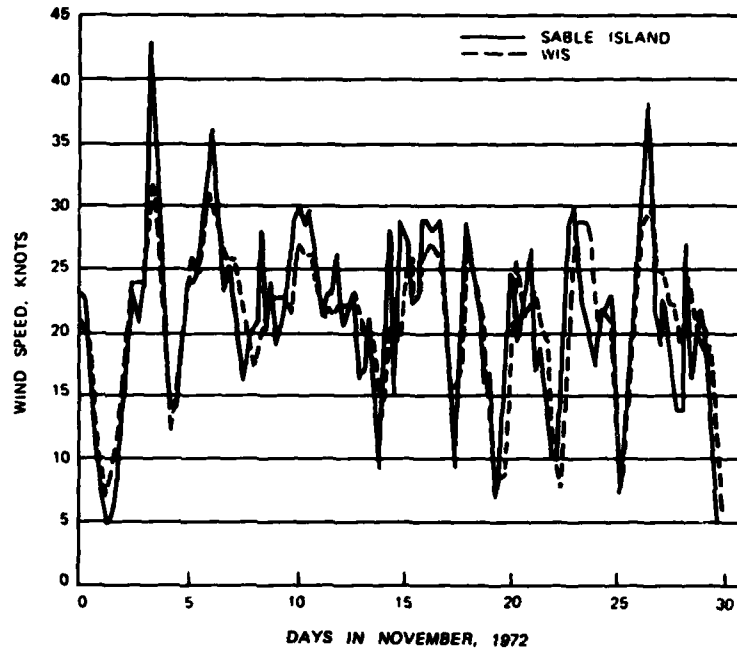


Figure B5. Comparison of hindcast (WIS) and measured (Sable Island) wind speed at Sable Island for November 1972

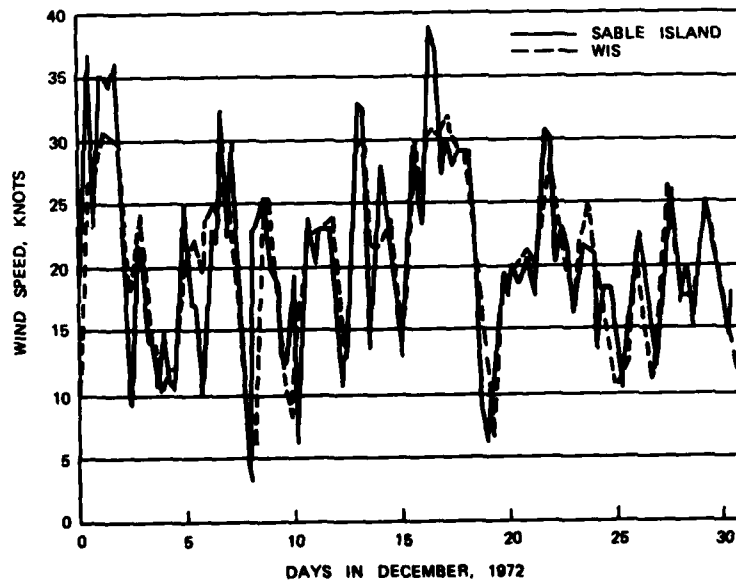


Figure B6. Comparison of hindcast (WIS) and measured (Sable Island) wind speed at Sable Island for December 1972

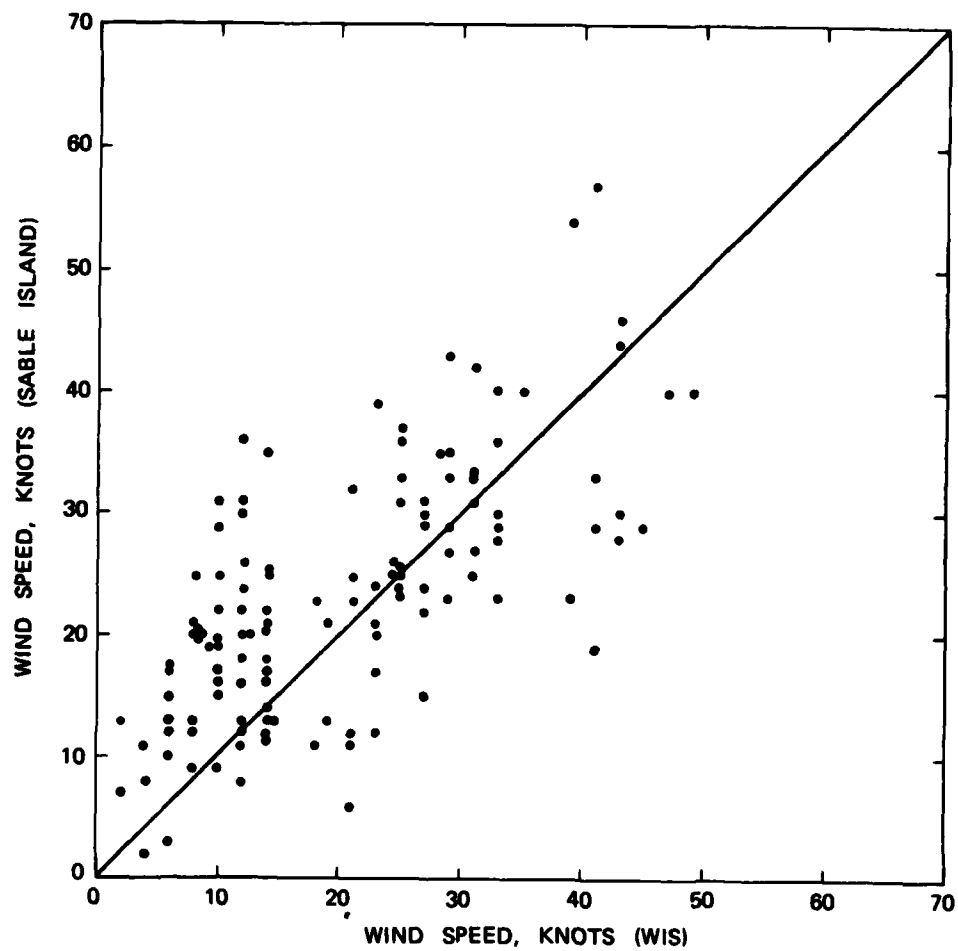


Figure B7. Cross plot of hindcast (WIS) and measured (Sable Island) wind speeds at Sable Island for January 1972

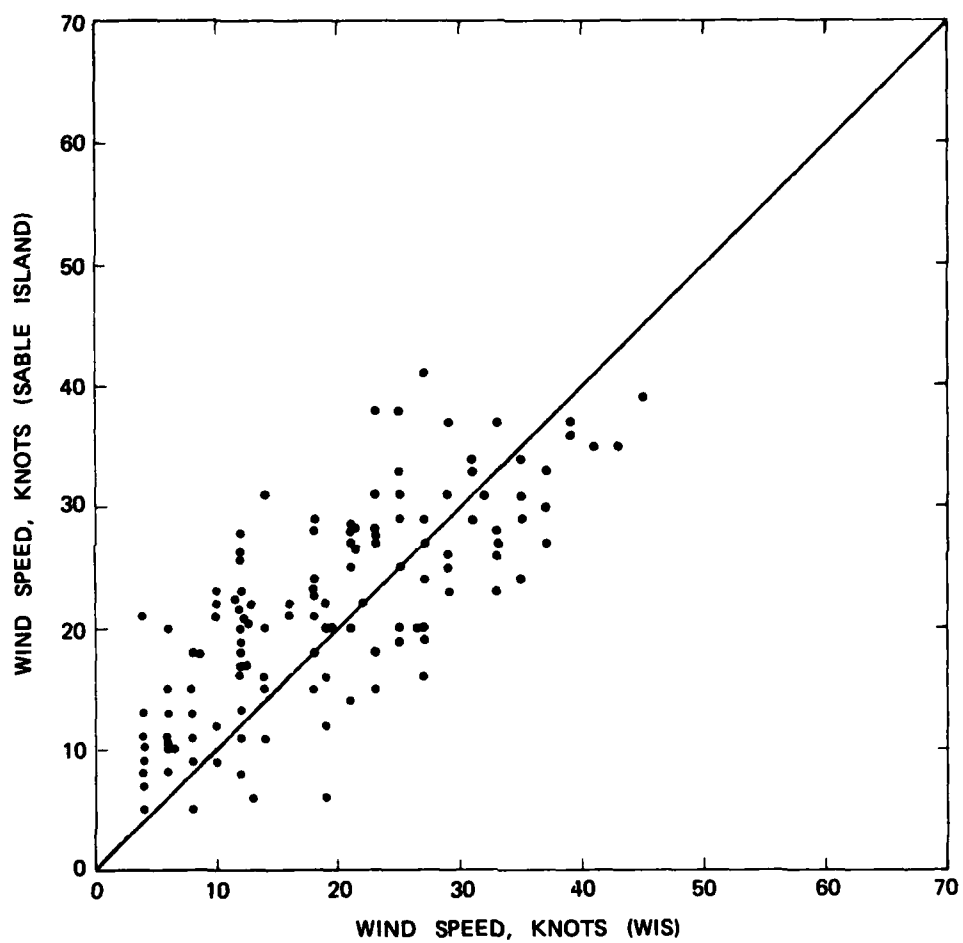


Figure B8. Cross plot of hindcast (WIS) and measured (Sable Island) at Sable Island for March 1972

Island (Figure B9). As shown in Figure B9, the computed high winds are very similar to the measured wind speeds, and the means of both data sets are nearly identical.

5. In Appendix A, a somewhat heuristic argument was presented in favor of using a complete simulation of the planetary boundary layer in the estimation of surface winds from geostrophic-level winds. A past alternative to this has been to use simple algorithms to represent such wind relations. Typically, this approach is justified on the grounds that a more thorough treatment is not merited due to inherent errors in the input specifications. As shown in Appendix A, such an argument is not very persuasive, since any additional bias introduced by an incorrect wind model will add to any existing random errors and biases in the wind parameters specified at the top of the boundary layer. The ultimate goal must be to achieve maximum accuracy in the specification of the geostrophic-level winds and the derived surface-level winds. Figure B10 presents a comparison of the characteristic behavior of a similarly based planetary boundary layer model to a simple linear algorithm that is still used in different engineering and scientific applications today. The factor "R" referenced in this figure is somewhat a "tuning coefficient" and usually the value selected is referenced as being slightly greater than 1. As shown in Figure B10, one would expect that a linear relation will significantly overpredict extreme wind conditions. To test this hypothesis, winds off magnetic tapes from Fleet Numerical Weather Central (FNWC)* were compared with the same measured winds at Sable Island as were computed winds from the present study. The hind-cast winds in this comparison were estimated using a simple algorithm rather than a complete boundary layer model. As shown in Figure B11, there is a significant, consistent overprediction at high wind speeds.

6. Comparisons to the NDBO buoys (EB01, EB13) contain wind speed and direction parameters. Some of the buoy data, although plotted as valid data, probably represent equipment problems, especially some of

* The methodology employed to compute the winds for FNWC was developed by Meteorological International, Incorporated (MII) and is discussed in Holl and Mendenhall 1971.

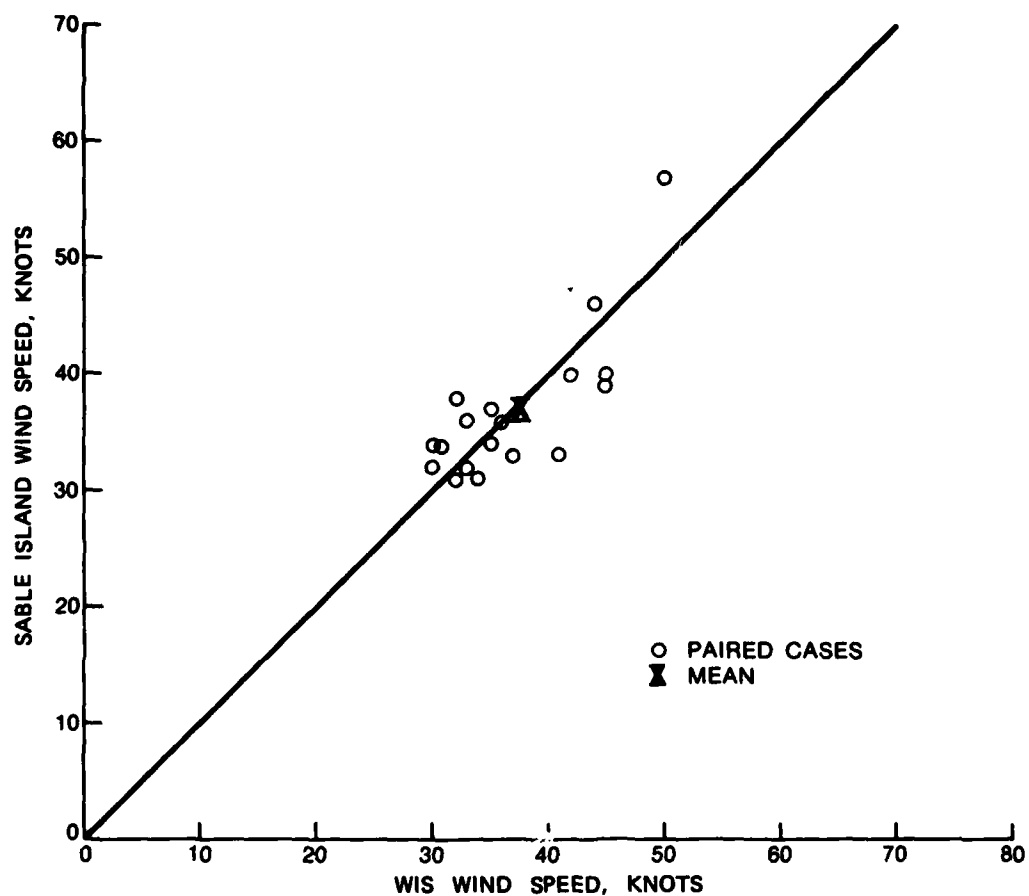


Figure B9. Cross plot of time-paired hindcast (WIS) and measured (Sable Island) wind speeds from January and March 1972 for observations at Sable Island exceeding 30 knots

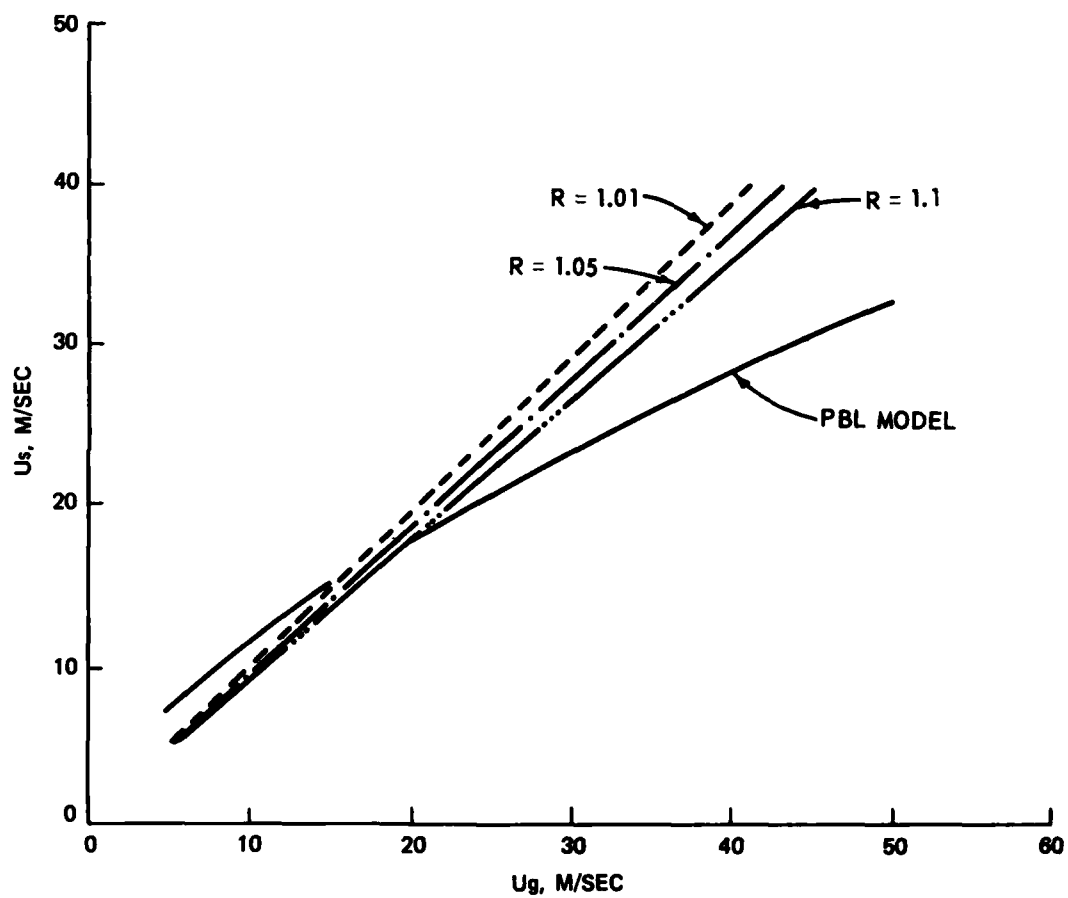


Figure B10. Surface wind, U_s , as a function of geostrophic wind, U_g , PBL theory and from a simple linear algorithm with various tuning coefficients (R)

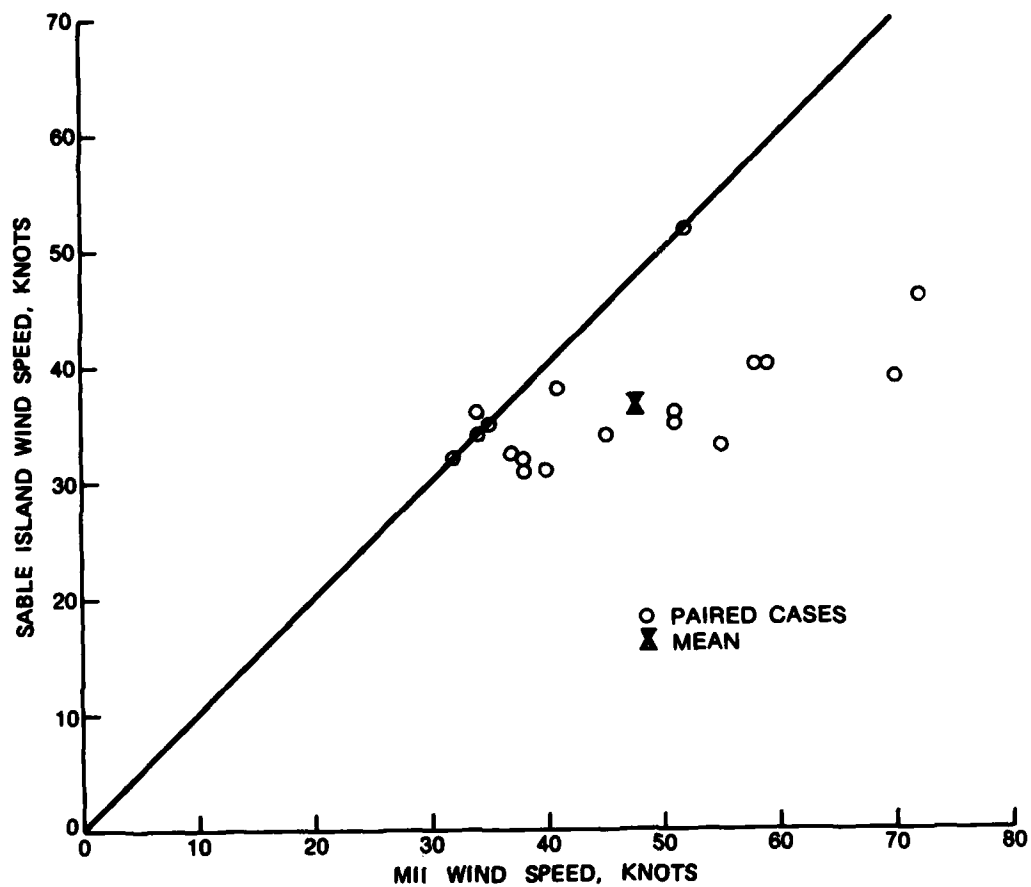


Figure B11. Cross plot of hindcast (MII) and measured (Sable Island) wind speeds from January and March of 1972 for observations at Sable Island exceeding 30 knots

the zero-wind conditions. In spite of this, the time series plots of predicted* (WIS) and measured (buoy EB01 or EB13) wind speeds show the predicted winds to be very similar to the measured winds. Likewise, the time series plots of direction differences indicated expected variance with most of the larger differences occurring at low wind speeds (Figures B12-B20).

7. Figure B21 presents comparison statistics of measured (buoy) and computed wind speeds for all available months. The random error (approximated by root-mean-square-error, RMSE) and bias are sufficiently small that they are not expected to significantly affect the statistical characteristics of the hindcast waves.

8. The specific comparisons provide descriptions of the response of the wind hindcast procedure (model) to the supplied input (pressure gradients, etc.) for specified times and locations. Since the model can hindcast winds similar to measured winds in the specified areas, the model is expected to provide reliable results in areas where no comparative data are available.

* For these comparisons, the WIS winds were transferred to the 10-m level of the buoy anemometers.

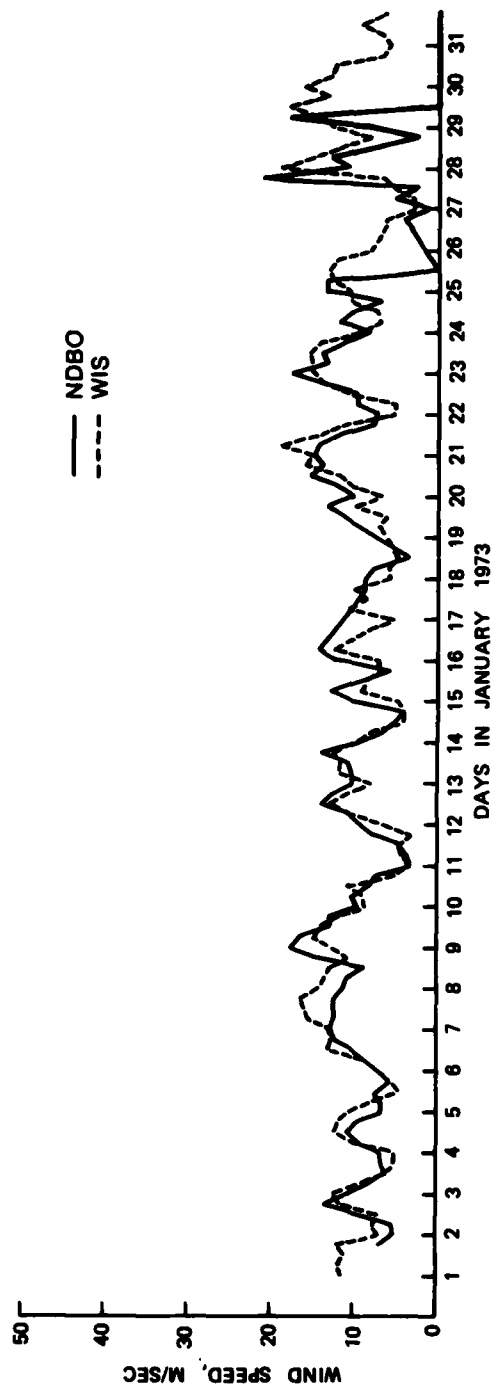
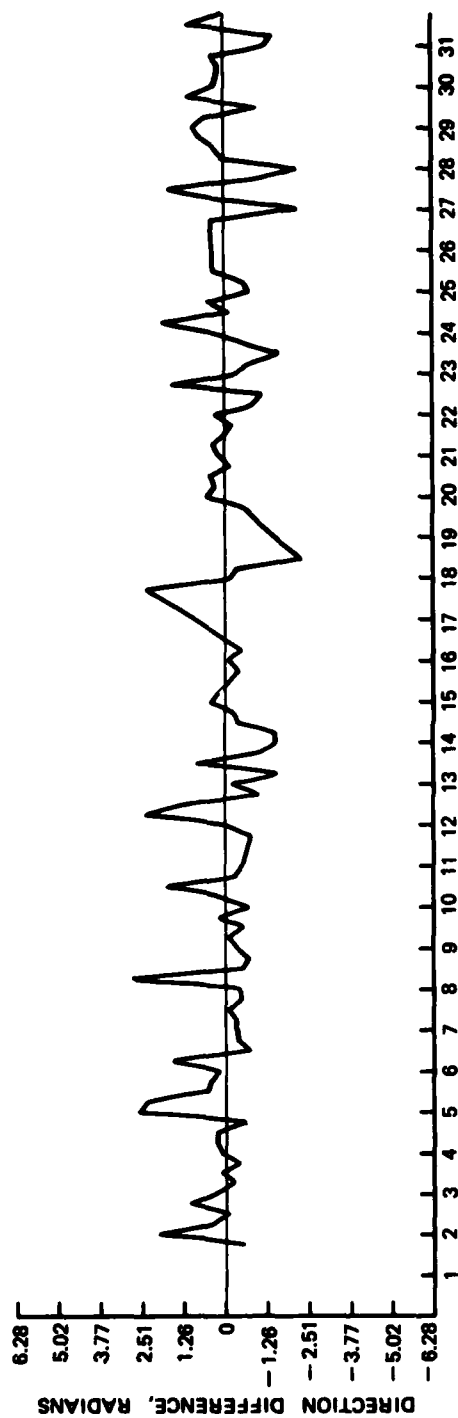


Figure B12. Comparison of NDBO and WIS wind data for January 1973 at EB01

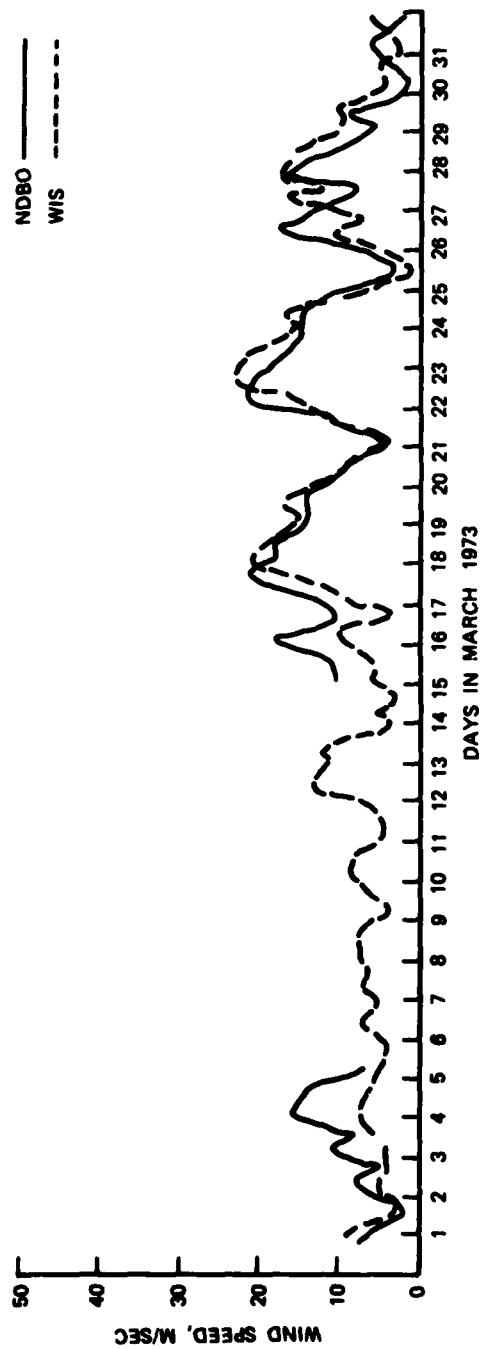
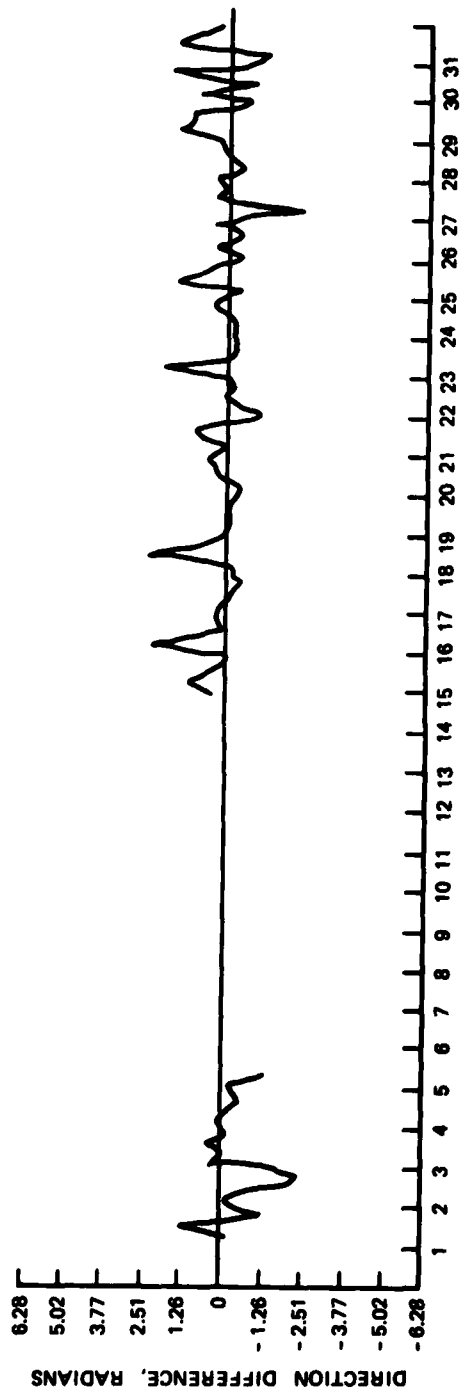


Figure B13. Comparison of ND80 and WIS wind data for March 1973 at EB01

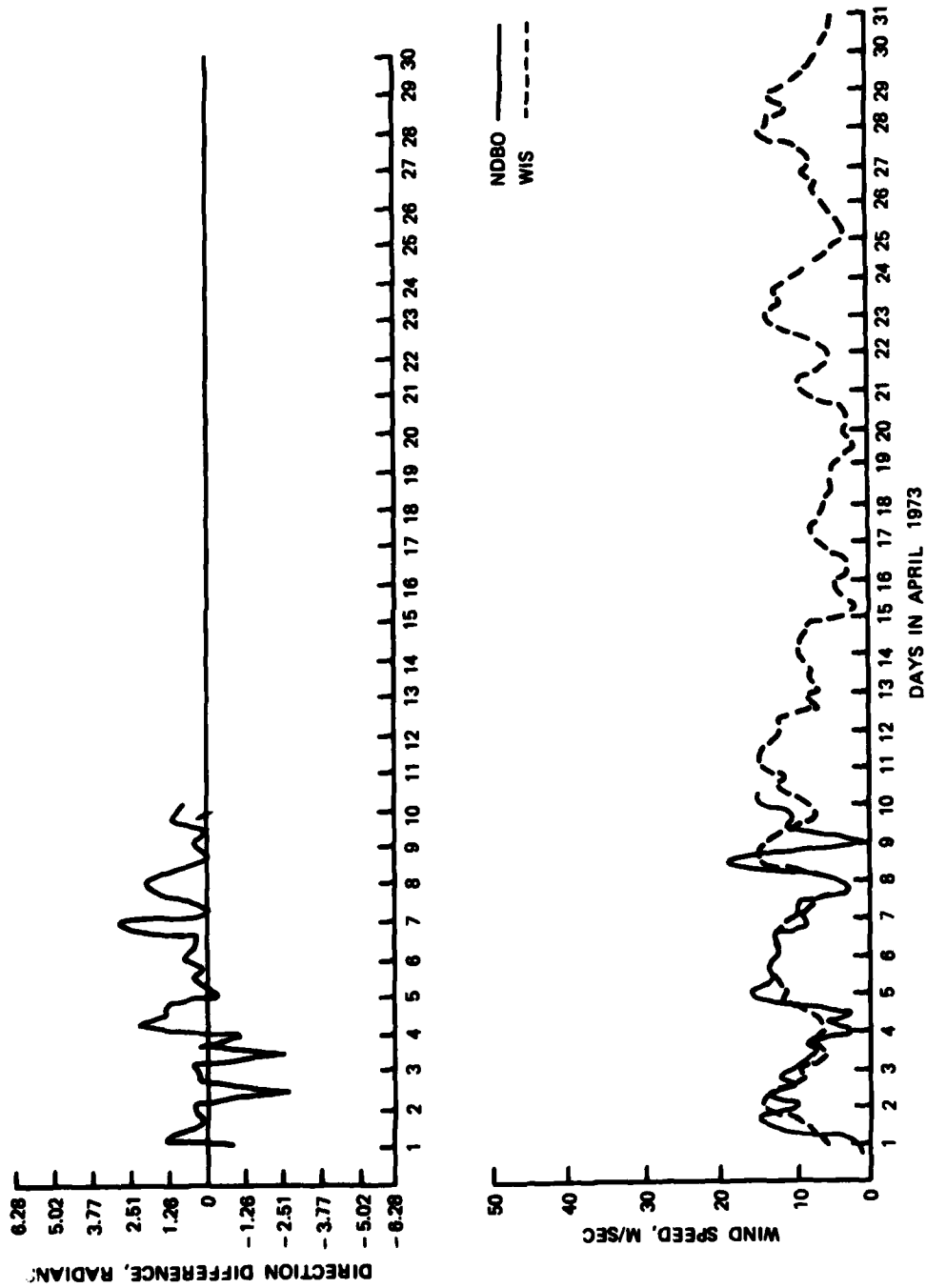


Figure B14. Comparison of NDBO and WIS wind data for April 1973 at EB01

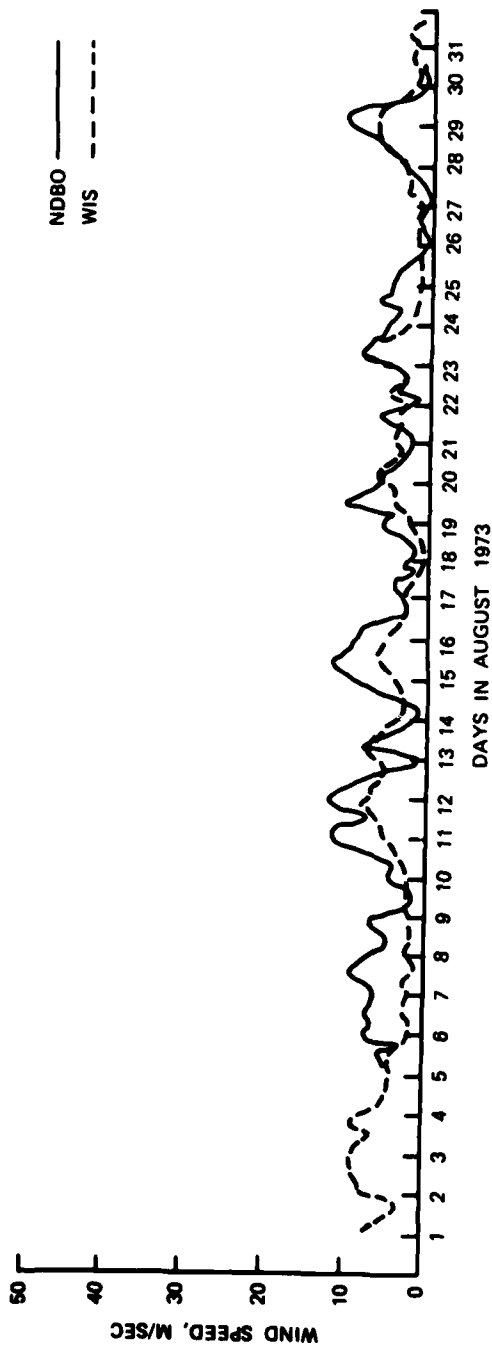
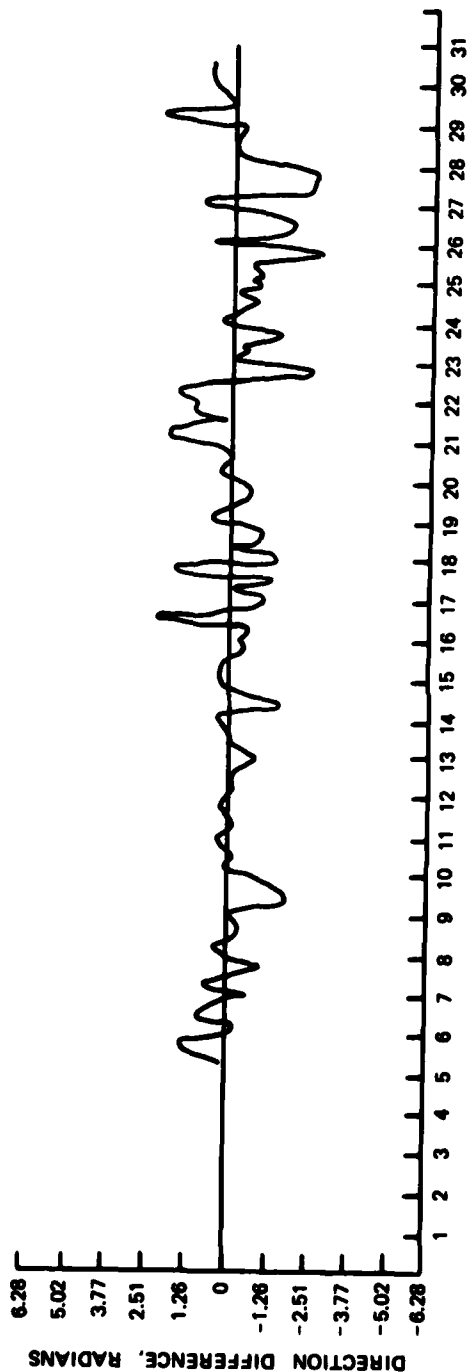


Figure B15. Comparison of ND80 and WIS wind data for August 1973 at EB01

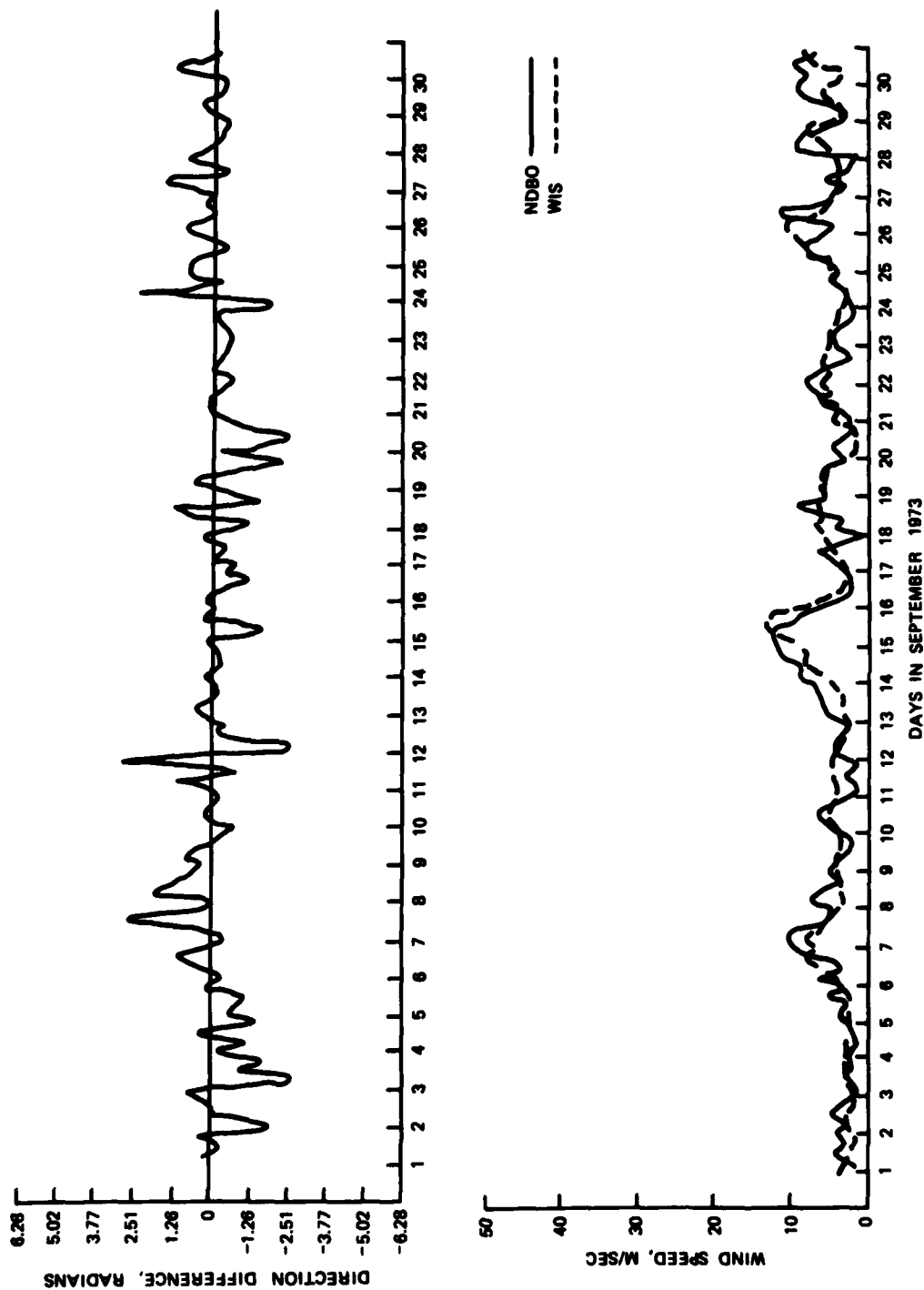


Figure B16. Comparison of NDBO and WIS wind data for September 1973 at EB01

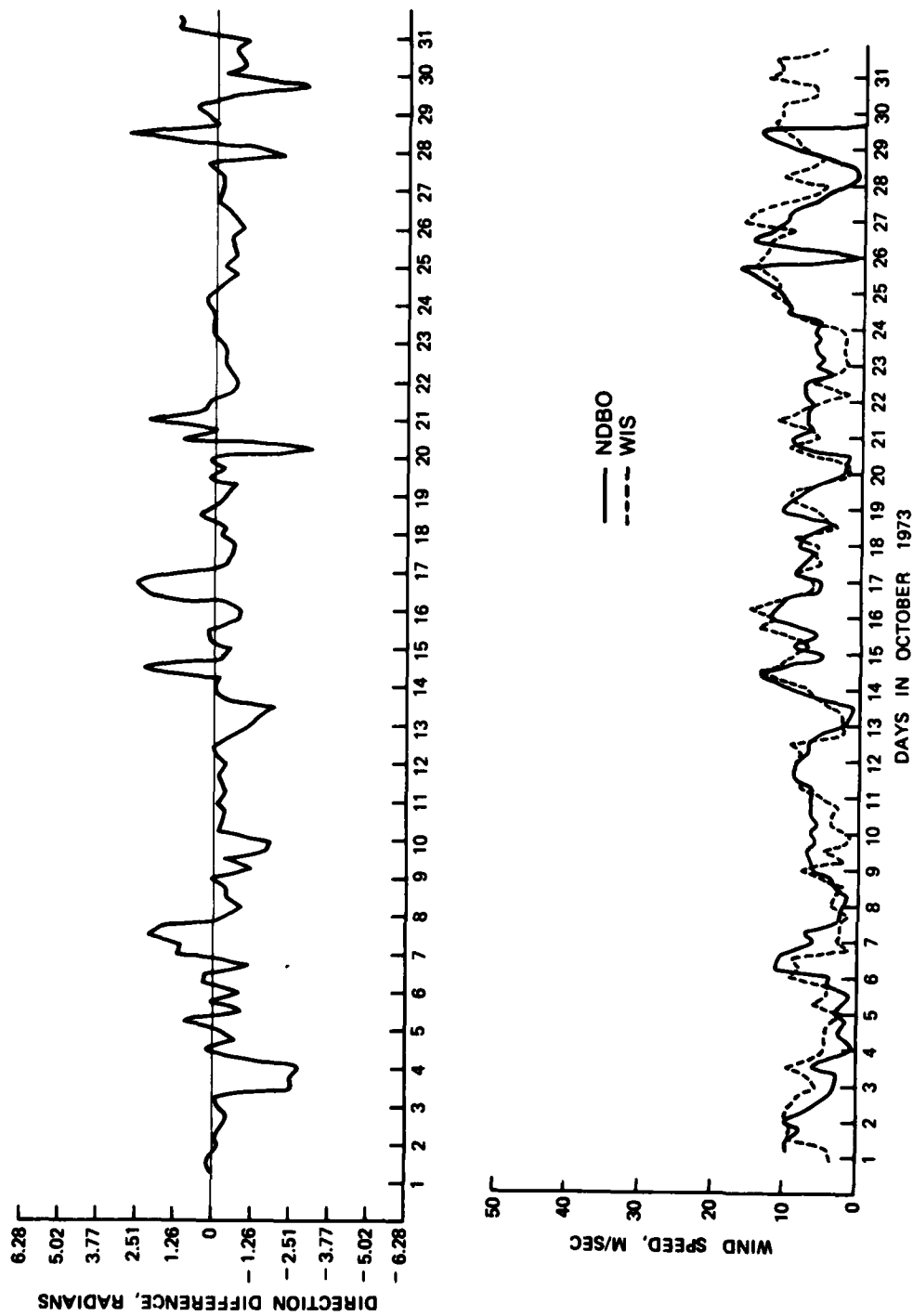


Figure B17. Comparison of NDBO and WIS wind data for October 1973 at EB01

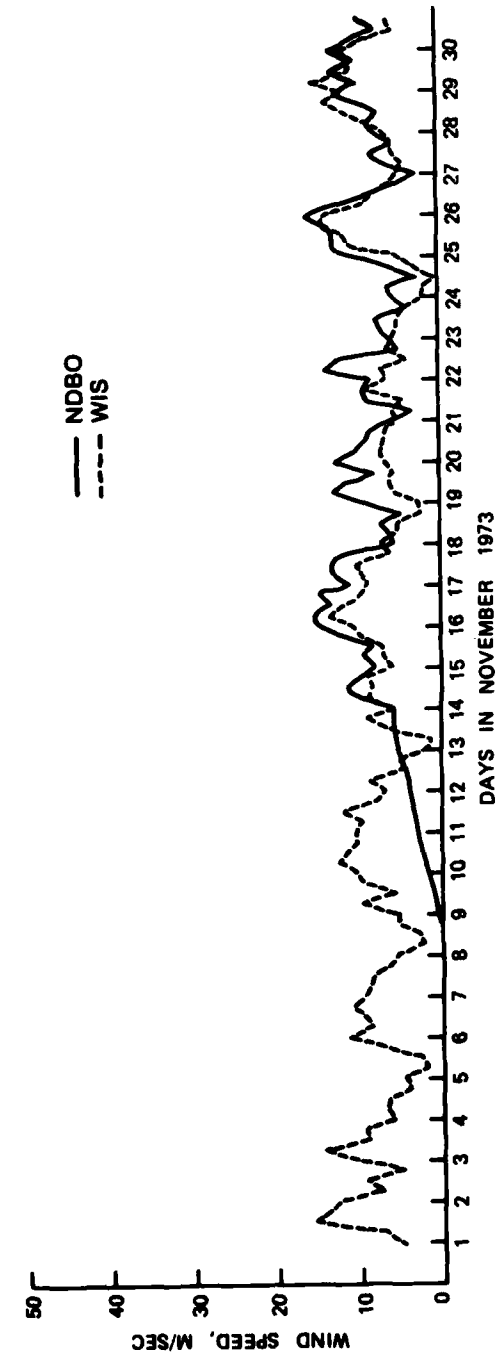
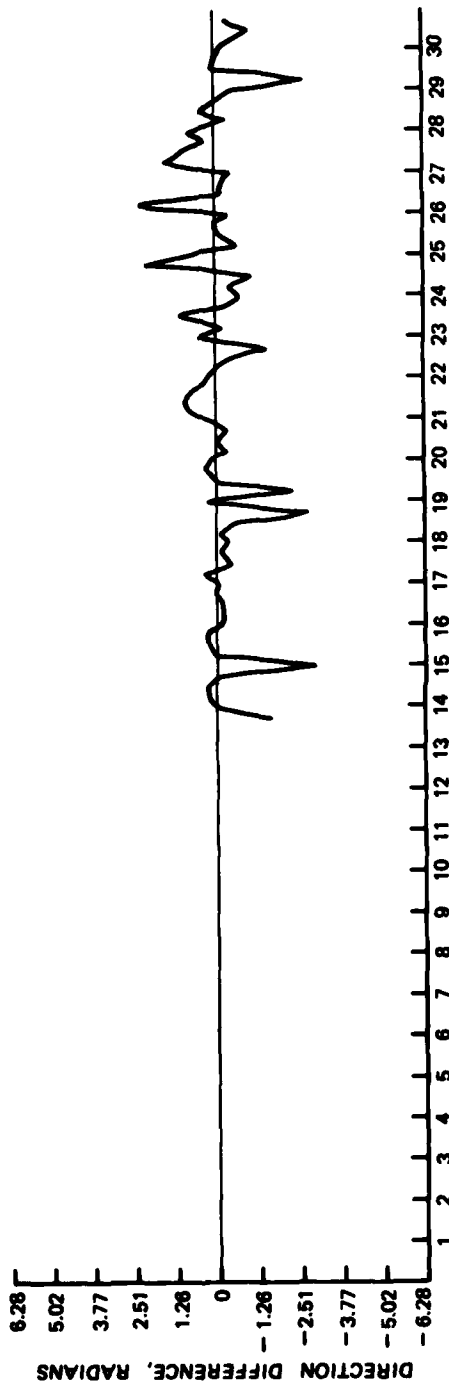


Figure B18. Comparison of NDBO and WIS wind data for November 1973 at EB01

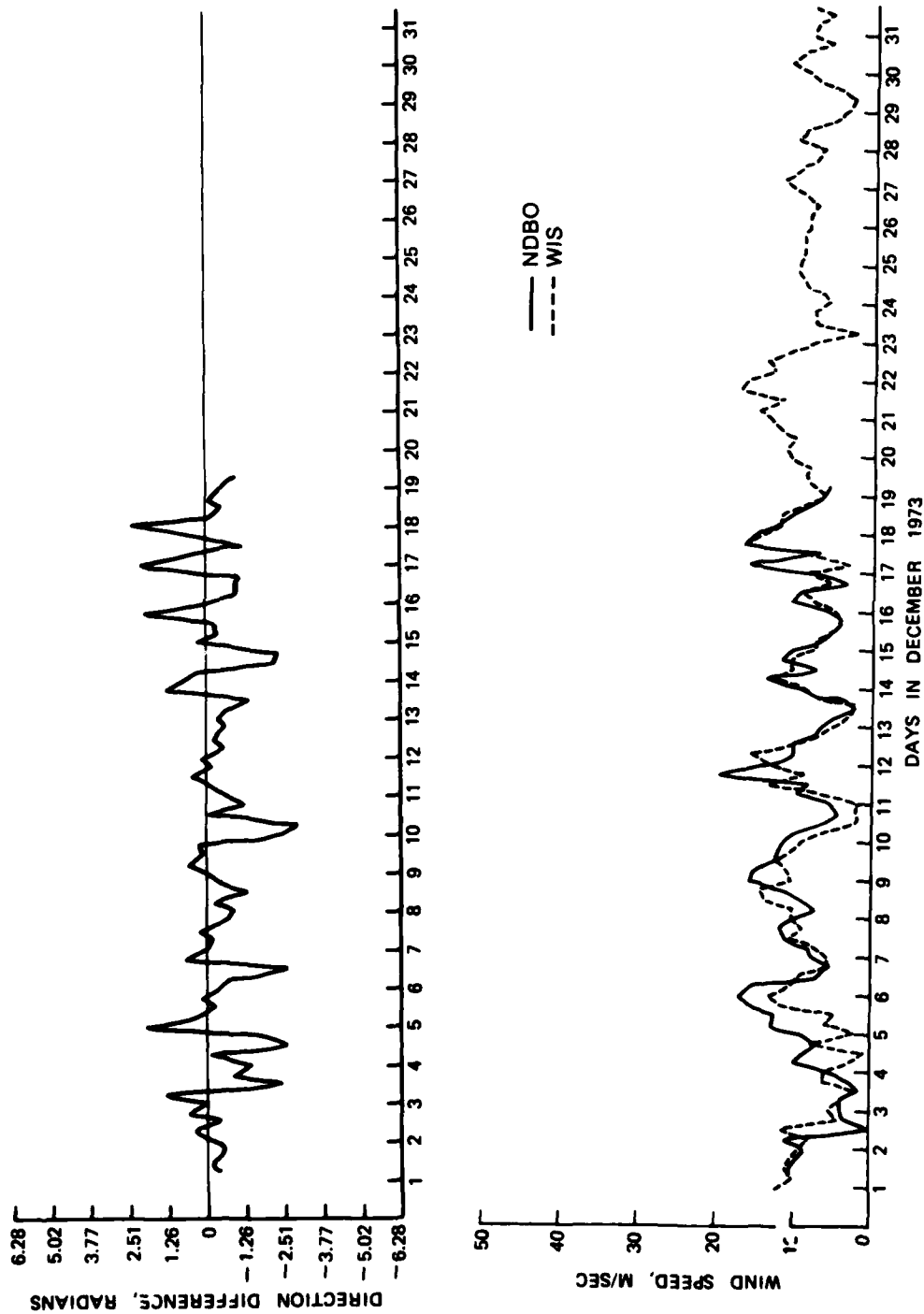


Figure B19. Comparison of NDBO and WIS wind data for December 1973 at EB01

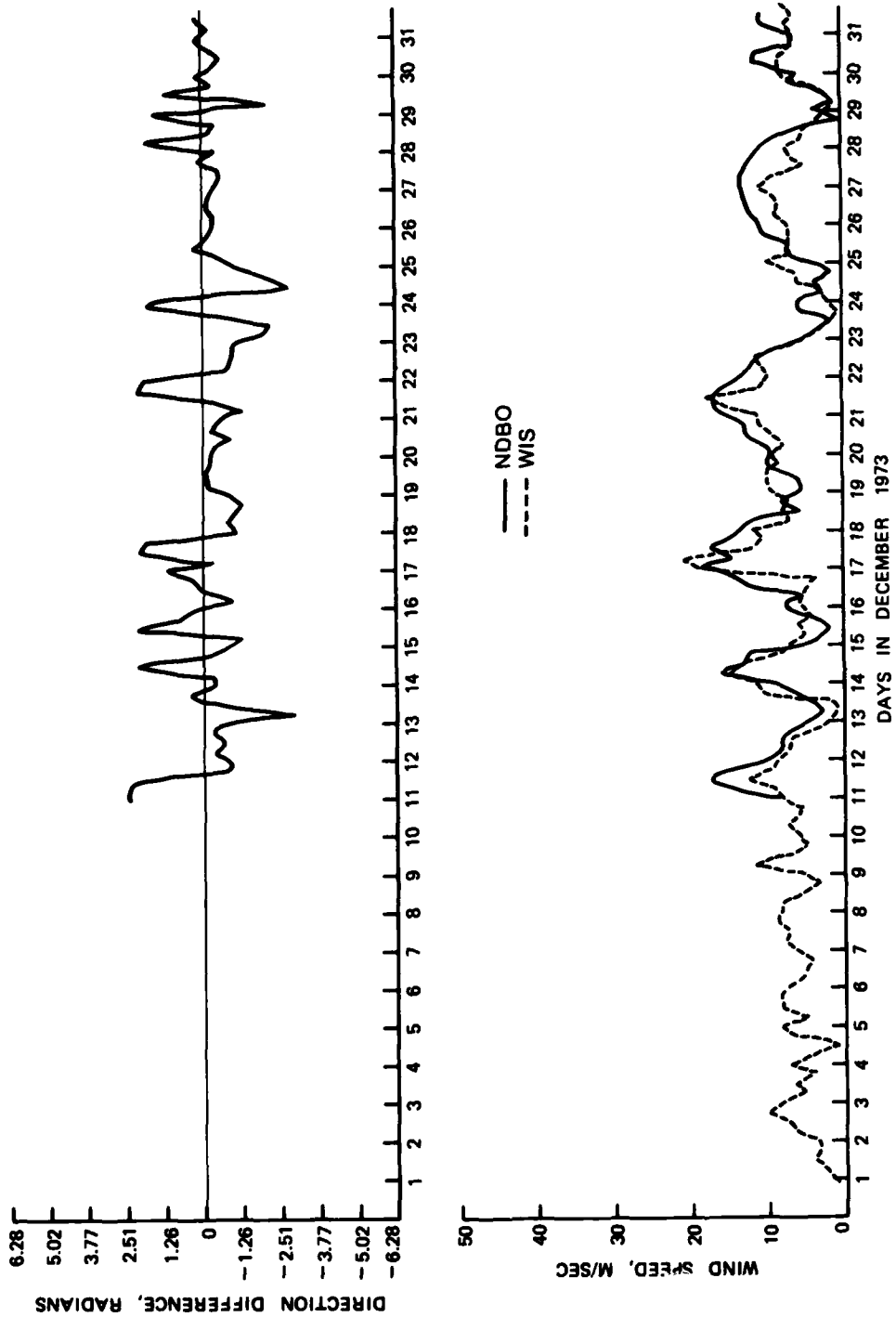


Figure 20. Comparison of NDBO and WIS wind data for December 1973 at EB13

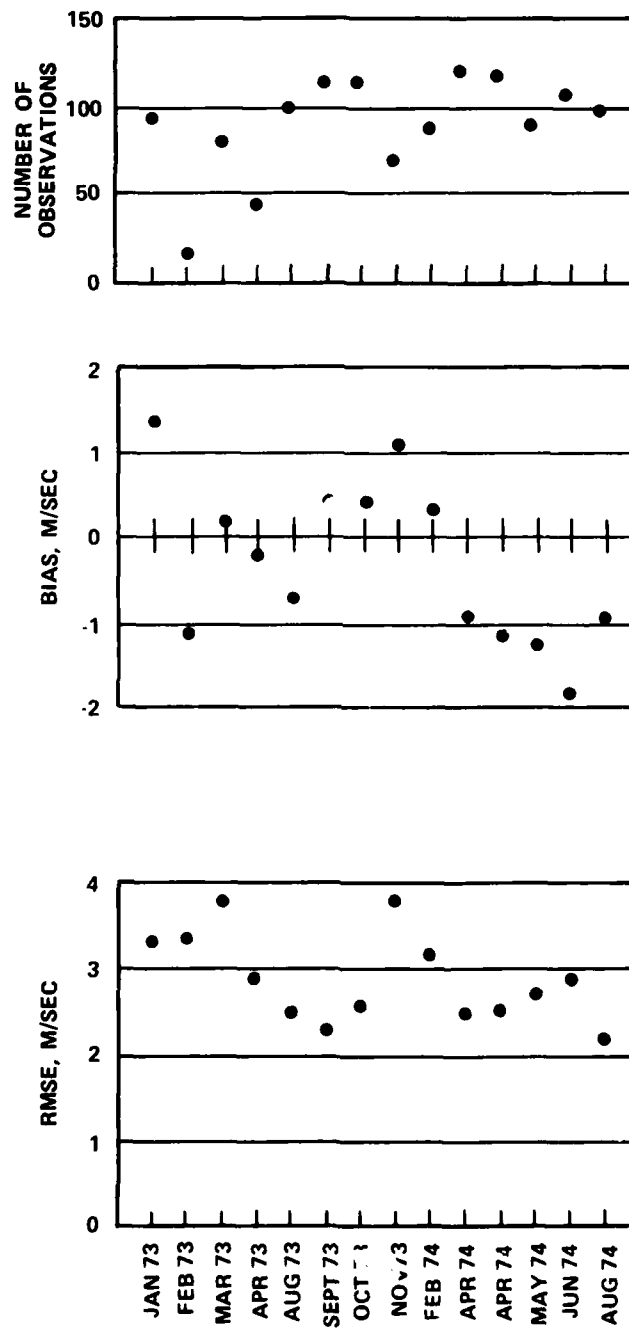


Figure B21. Comparative statistics for WIS wind data and corresponding NDBO buoy data

In accordance with letter from DAEN-RDC, DAEN-ASI dated 22 July 1977, Subject: Facsimile Catalog Cards for Laboratory Technical Publications, a facsimile catalog card in Library of Congress MARC format is reproduced below.

Resio, D.T.

Objective specification of Atlantic Ocean wind fields from historical data / by D.T. Resio, C.L. Vincent, W.D. Corson (Hydraulics Laboratory, U.S. Army Engineer Waterways Experiment Station). -- Vicksburg, Miss. : The Station ; Springfield, Va. : available from NTIS, 1982.

50 p. in various pagings ; ill. ; 27 cm. -- (WIS report ; 4)

Cover title.

"May 1982."

"Prepared for Office, Chief of Engineers, U.S. Army."

"Wave Information Studies of U.S. Coastlines."

Bibliography: p. 25.

1. Atlantic Ocean. 2. Mathematical models.
3. Numerical analysis. 4. Ocean waves. 5. Wind waves.
I. Vincent, C.L. II. Corson, W.D. III. United States.
Army. Corps of Engineers. Office of the Chief of Engineers.

Resio, D.T.

Objective specification of Atlantic Ocean : ... 1982.
(Card 2)

IV. Wave Information Studies of U.S. Coastlines.

V. U.S. Army Engineer Waterways Experiment Station.

Hydraulics Laboratory. VI. Title VII. Series: WIS

report (U.S. Army Engineer Waterways Experiment Station) ; 4.
TA7.W349 no.4

**DATE
FILMED**

8-8